

L I C E N C E T O M c M A S T E R U N I V E R S I T Y

This THE.SIS has been written
[Thesis, Project Report, etc.]

by CHERYL ANN SEKINE for
[Full Name(s)]

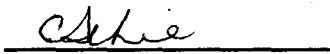
Undergraduate course number GEOLOGY 7K06 at McMaster
University under the supervision/direction of DR. J. R. KRAMER

In the interest of furthering teaching and research, I/we hereby grant to
McMaster University:

1. The ownership of 5 copy(ies) of this
work;
2. A non-exclusive licence to make copies of
this work, (or any part thereof) the
copyright of which is vested in me/us, for
the full term of the copyright, or for so long
as may be legally permitted. Such copies
shall only be made in response to a written
request from the Library or any University
or similar institution.

I/we further acknowledge that this work (or a surrogate copy thereof) may
be consulted without restriction by any interested person.


Signature of Witness,
Supervisor


Signature of Student

JUNE 11/96
date

(This Licence to be bound with the work)

THE EQUATORIAL PACIFIC CARBON MODEL
(EPCM)

The Equatorial Pacific Carbon Model (EPCM)

by

Cheryl A. Sekine

A Thesis

Submitted to the Department of Geology
in Partial Fulfilment of the Requirements for the
Degree Bachelor of Science

McMaster University

April, 1996

BACHELOR OF SCIENCE, (1996)
(Honours Science, Complementary Studies)

McMaster University,
Hamilton, Ontario

TITLE: The Equatorial Pacific Carbon Model

AUTHOR: Cheryl A. Sekine

SUPERVISORS: Dr. J.R. Kramer and Dr. Imre Takacs

Abstract

A computer simulated model representing carbon dynamics within the eastern equatorial Pacific was developed. The three compartment model incorporated the physical, biological and chemical processes most significant to the region of study representing both “normal” and highly disruptive conditions. The events which interrupt the normal carbon dynamics are known as El Niño events. The most profound effects that the El Niño has on the eastern equatorial Pacific are anomalously high sea-surface temperatures and a weakening in the typically intense upwelling motion. It is during these periods that the equatorial Pacific has been thought as being a sink for carbon dioxide. The EPCM incorporated these extreme changes, as typified by sea-surface temperature and upwelling, in order to determine the levels of sensitivity of the model parameters to these adverse conditions. The EPCM suggests that variations in upwelling rates have a much greater effect on model parameters than a change in sea-surface temperatures. As well, it has been suggested that cooler temperatures limit zooplankton and phytoplankton parameters much more than warmer conditions. Lastly, it has been demonstrated that, according to the EPCM, the equatorial Pacific is always a source of carbon dioxide to the atmosphere. Net movement towards the atmosphere persists even during periods when upwelling is at its weakest, as simulated by the EPCM.

ACKNOWLEDGMENTS

I would like to give sincere thanks to Dr. Kramer for supervising me throughout this project and for providing me with invaluable experiences that will be useful in the years to come.

I would also like thank Dr. Imre Takacs, of Hydromantis, for all of the help with GPS-X . I surely could not have finished this project without him!

Thanks to everyone in 405 for all of their scholastic and “mental” support, and simply for making me laugh during those completely stressed-out days.

Special thanks to the two best friends a person could ever have. The support and love that Jason Galindo and Jennifer Roy have both given me has taught me what true friendship is all about.

Last, but never least, I dedicate this thesis to my parents who are always there caring for me no matter what *mood* I am in. I love you both!

TABLE OF CONTENTS

Abstract	ii
Acknowledgments	iii
List of Figures	iv
◆ Introduction	1
(1) Model Layout	5
• Location of Study Area	5
• Compartment Characterization	6
(2) Description of Model Processes	8
• Biological Cycling Within the Surface Layer	8
• Phytoplankton Growth Rate	10
• Phytoplankton Death Rate	15
• Zooplankton Growth Rate	17
• Zooplankton Death Rate	18
• Zooplankton Excretion Rate	18
(3) Transfer Mechanisms	20
• Horizontal Advection: The Equatorial Currents	21
• Upwelling	23
• Downwelling or Sinking	24
• Flux Between the Surface and the Local Atmospheric Layers	25
• Flux Between the Local Atmosphere and the Rest of the Earth's Atmosphere	28
(4) The Peterson's Matrix	30
• General Introduction to the Peterson's Matrix	30
• The Peterson's Matrix with respect to the EPCM	30
• Reaction Rates	32
• Mass Balances	33
(5) Description of Model Runs and Results	34
• Steady-State	34
• Sensitivity Analysis	37
- El Niño	37
- Temperature Effects	40
- Upwelling Effects	52
• Historic Runs	58
• Business as Usual - A Look into the Foreseeable Future	60

(6) Discussion and Conclusions	63
(7) References	68
Appendix A: Table 1 - EPCM variables	
Appendix B: Table 2 - EPCM Constants	
Appendix C: Table 3 - EPCM Steady-Stocks - New Initial Values	
Appendix D: GPSx - ACSL Model Code	

LIST OF FIGURES

Figure 1: Location of study region	5
Figure 2: Schematic of the study region dimensions	6
Figure 3: Schematic of the EPCM subsystems	8
Figure 4: Diagram showing depth versus productivity as a function of light intensity. Productivity is inhibited at the surface and is maximum where light intensities are less.	12
Figure 5: Half-saturation curve	14
Figure 6: Transfer mechanisms of the EPCM	20
Figure 7: Currents of the Equatorial Pacific	21
Figure 8: Upwelling processes in the open equatorial Pacific Ocean	22
Figure 9: Peterson's Matrix for the EPCM	31
Figures 10a to 10b: Determination of the steady-state values for each of the component concentrations	35-36
Figure 11a: Phytoplankton growth rate as a function of sea-surface temperature	41
Figure 11b: Phytoplankton death rate as a function of sea-surface temperature	42
Figure 11c: Upwelling rate of phytoplankton as a function of sea-surface temperature	42
Figure 11d: Surface phytoplankton concentrations as a function of sea-surface temperature	43
Figure 12a: Zooplankton growth rate as a function of sea-surface temperature	44
Figure 12b: Zooplankton death rate as a function of sea-surface temperature	44
Figure 12c: Upwelling rate for zooplankton as a function of sea-surface temperature	45
Figure 13a: Upwelling rate for nutrients as a function of sea-surface temperature	46
Figure 13b: Surface nutrient concentrations as a function of sea-surface temperature	46
Figure 14a: Zooplankton excretion rate as a function of sea-surface temperature	47
Figure 14b: Surface organic carbon concentrations as a function of sea-surface temperature	48
Figure 15a: Atmospheric CO ₂ concentration as a function of sea-surface temperature	51
Figure 15b: Upwelling rate for CO ₂ as a function of sea-surface temperature	51
Figure 15c: CO ₂ ocean-atmosphere flux as a function of sea-surface temperature	52
Figure 16a: Phytoplankton growth rate as a function of upwelling velocity	53
Figure 16b: Zooplankton excretion rate as a function of upwelling velocity	54
Figure 16c: Surface nutrient concentration as a function of upwelling velocity	55
Figure 16d: CO ₂ ocean-atmosphere flux as a function of upwelling velocity	55
Figure 16e: Atmospheric CO ₂ partial pressure as a function of upwelling velocity	57

Figure 17a: EPCM forcing variables: CO ₂ concentration in the external atmosphere and sea-surface temperature - 1900 to 2020	58
Figure 18a: Ocean-atmosphere flux 1900 to 2020	62
Figure 18b: pCO ₂ and H ₂ CO ₃ predictions 1900 to 2020	62

EQUATORIAL PACIFIC CARBON MODEL (EPCM)

INTRODUCTION

In recent years it has been hypothesized that the earth's oceans contribute to the global carbon cycle by acting as a sink for atmospheric carbon dioxide (*Siegenthaler and Sarmiento, 1993; De Baar and Suess, 1993*). However, this idea has been debated among scientists (*Smith and Hollibaugh, 1993; Longhurst, 1991*). A complete understanding of the oceanic role with respect to atmospheric carbon dioxide levels requires the comprehension of carbon cycling in isolated oceanic areas.

The equatorial Pacific is a unique oceanic region in that it is a site of intense upwelling. Upwelling is a process by which deep water is transferred to the ocean surface where there exists a divergent water flow. According to continuity, insufficient water of an area must be replaced. In the Pacific Ocean, near the equator, the South Equatorial Current is the principle surface flow in which divergence away from the equator occurs due to the rotation of the Earth. Consequently, this water deficit is fulfilled by the upwelling process, transporting cold, carbon dioxide (CO₂) and nutrient rich water from the deep ocean to the surface layer. Thus, the high CO₂ concentration established within the surface layer has created the delineation of the equatorial Pacific as being the largest natural ocean source of CO₂ to the atmosphere (*Murray et al., 1994*), having a

flux estimate in the vicinity of 0.9 gigatons (Gt) of carbon per year (*Gammon et al., 1985 from Murray et al., 1994*).

However, deviations in atmospheric CO₂ levels from the norm have been observed. These perturbations are principally produced by El Niño/Southern Oscillation (ENSO) events. This is a coupled ocean-atmosphere process that gives rise to characteristic responses in the ocean and the atmosphere causing short-term climatic changes. In the eastern equatorial Pacific specifically, ENSO acts to weaken upwelling and create warmer sea-surface temperatures which subsequently decreases biological productivity and declines the concentration of nutrients and CO₂ in the surface waters (*Barber and Chavez, 1986; Ramage, 1986; Feely et al., 1987; Murray et al., 1994*). Consequently, it has been considered that during ENSO events the equatorial Pacific acts as a sink for CO₂.

The integrated mechanisms influencing carbon cycling within the equatorial Pacific requires that the physical, chemical and biological attributes of the system be considered simultaneously. There has been extensive research on, and data collection of (*Murray et al., 1994; Gouriou and Toole, 1993; Feely et al, 1987, 1994; Picaut and Tournier, 1991*) the individual components of this region, but little attention has been given to modelling of the equatorial Pacific as a whole. Elsewhere, integrative efforts have been put forth in the modelling of phytoplankton populations within various aquatic ecosystems. Di Toro et al. (*1971*) modelled the phytoplankton population of the Sacramento - San Joaquin Delta with respect to nutrient concentrations. The processes, in relation to

zooplankton, phytoplankton and nutrient concentrations, found within the Di Toro system are the major parameters affecting carbon cycling within the equatorial Pacific. This model exhibits how the death and growth rates of the phytoplankton and zooplankton contribute to the carbon pool of their environment with temperature, solar radiation and nutrient availability limiting the process rates.

Di Toro et al. (1971) incorporated the advective flow of water as a transport parameter into the model. The concentration of each of the components is, thus, altered by their corresponding input and output concentrations. However, according to Murray et al. (1994) it is the physical, rather than the biological processes, that ultimately control the cycling of CO₂ within the equatorial Pacific. Thus, accurate simulation of the carbon fluxes and concentrations of this area requires other characteristic transport mechanisms to be represented within an integrated model. The circulation of the tropical Pacific Ocean has been investigated by Philander et al. (1987). This study shows that the dynamics of the water follows four routes. The Equatorial Undercurrent, which travels below the thermocline, flows towards the equator supplying water for upwelling to the surface. The main mode of horizontal transport at the surface is the South Equatorial Current. The surface water is consequently forced away from the equator to higher latitudes. As mentioned previously, water from the deep is upwelled with a tremendous magnitude. In addition, to counterbalance the excess surface waters there is a small downwelling flux from the surface to the deep ocean.

The cycling of nutrients is essential for the comprehension of the circulation of carbon (*Fasham et al., 1990*), particularly within the high nutrient regime of the equatorial Pacific. The interaction of plankton and nitrogen in the upper ocean has been modelled by Fasham et al. (1990). Nitrate is generally taken as the limiting nutrient of primary production (*Fielder et al., 1991*). Furthermore, the growth rate of phytoplankton is dependent on both nitrogen availability and the fecal pellets excreted by the zooplankton population contain a significant amount of nitrogen. Thus, “new” and “regenerated” production is stimulated by different forms of nitrogen (ie. nitrate and ammonium). A three dimensional, 2 layer box model of nitrate flux on a vertical and horizontal scale demonstrates that new production (ie. the net input of nitrate into the surface by horizontal and vertical advection) maintains the steady-state of nitrate via the loss of organic nitrogen through export production (*Fielder et al., 1991*).

I have developed the Equatorial Pacific Carbon Model (EPCM) in the hopes of satisfying various objectives. Firstly, the interactions within the equatorial Pacific must be understood as a unitary system. The EPCM will help in explaining how the biological, physical and chemical parameters and processes interact and contribute to the release of CO₂ into the atmosphere. In addition, the model makes it possible to determine the more sensitive parameters of the system in which comparisons may be made to the results of previous studies of the eastern tropical Pacific. The model will also make it possible to determine how atmospheric CO₂ levels have changed and predict what these level will be

like in the foreseeable future. However, the main challenge of the EPCM is to conclude whether the equatorial Pacific acts as a *net* sink or source of CO₂ to the atmosphere over a long-term scale.

(1) MODEL LAYOUT

Location of Study Area

The Equatorial Pacific Carbon Model (EPCM) considers an area in the eastern Pacific at 12° north to 12° south latitude and 97° west to 170° west longitude. Geographically, this is in the open ocean regions of the Pacific to the west of the Central American and Peru zones (*Figure 1*).

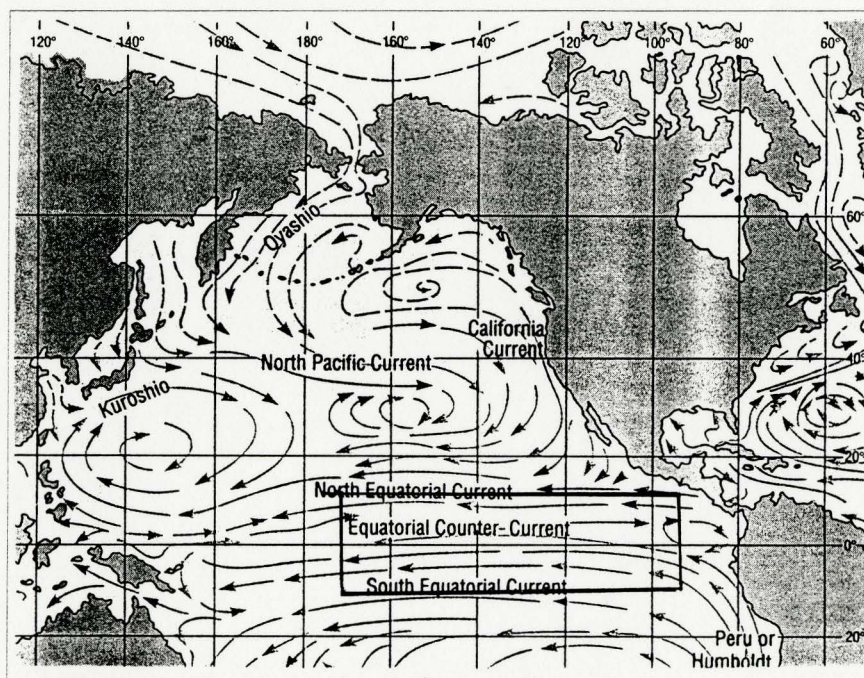


FIGURE 1. Location of study region.

The area of interest of the EPCM follows the sectioning similar to that defined in the Murray et al. (1994) study. Taken as a first approximation the total area of study is $4.31 \times 10^{13} \text{ m}^2$ (Figure 2)

Compartment Characterization

The model itself is separated into three distinct compartments for the entire area, as defined above. The ocean volume is divided two ways, consisting

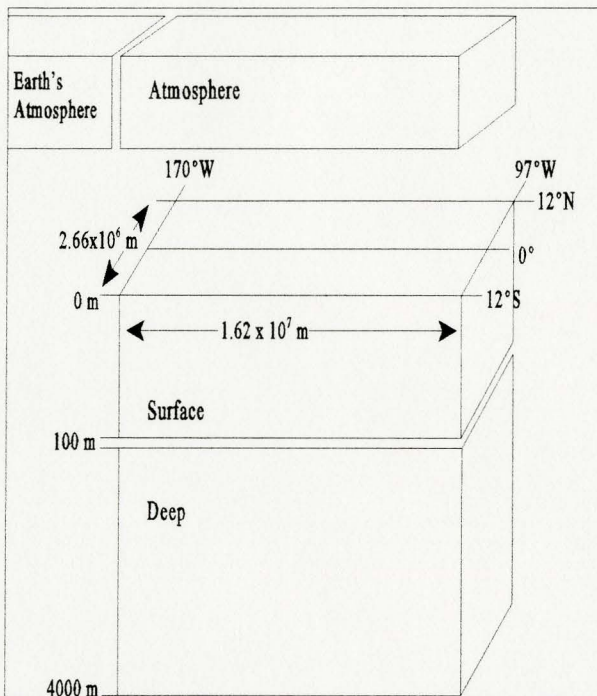


FIGURE 2: Schematic of the study region dimensions

of a surface or mixed layer and a deep layer. The surface layer is defined as being 100 m in depth which represents the average depth of the thermocline within the equatorial Pacific (Feely et al., 1987; Fielder et al., 1991). Thus, the volume of the surface layer has been taken as $4.3 \times 10^{15} \text{ m}^3$. The surface consists of the bulk of the activity within the EPCM, where productivity is the greatest (Parsons et al., 1984)

The surface layer is also important for the transfer of CO_2 into and out of the atmosphere depending on the CO_2 partial pressure difference between the surface layer and the overlying atmospheric box.

The mean span of the deep waters of the equatorial Pacific is 100 to 4000 m which encompasses a volume of $1.68 \times 10^{17} \text{ m}^3$. The deep ocean regions are much less dynamic with respect to biological cycling, . However, this layer is important for the mass movements of water and other materials, thus, affecting the surface concentrations. For example, the deep layer, (just below the thermocline) contains the nutrient reservoir, which is the nitrate supply for the upwelled water.

The atmospheric layer, above the oceanic compartments, is of the same area as that of the ocean (ie. $4.31 \times 10^{13} \text{ m}^2$). The single carbon species measured within the atmospheric layer is CO_2 or inorganic carbon. The CO_2 concentration within this compartment is key to the determination of the model objective of whether the equatorial Pacific acts as a net sink or source of atmospheric CO_2 .

Attached to the atmospheric compartment is an external atmospheric box representing the atmosphere for the remaining Earth outside of the equatorial atmosphere. The information contained within it is the annual mean CO_2 concentrations for greater than 100 years. This allows for the consideration of the rise in atmospheric CO_2 levels associated with the advent of the industrial revolution. The Earth's atmospheric compartment has been included in the EPCM so that the atmospheric layer will not accumulate excessive and unrealistic amounts of CO_2 .

(2) DESCRIPTION OF MODEL PROCESSES AND PROCESS RATES

Biological Cycling Within the Surface Layer

The EPCM considers five controlling subsystems as listed below:

- (1) Phytoplankton (PHYT)
- (2) Zooplankton (ZOO)
- (3) Nutrients (NUT)
- (4) Inorganic Carbon (CO₂)
- (5) Organic Carbon (ORGC)

Figure 3 is a schematic representation of all interactions in the model and include the 5 subsystems. The biological processes controlling the equatorial

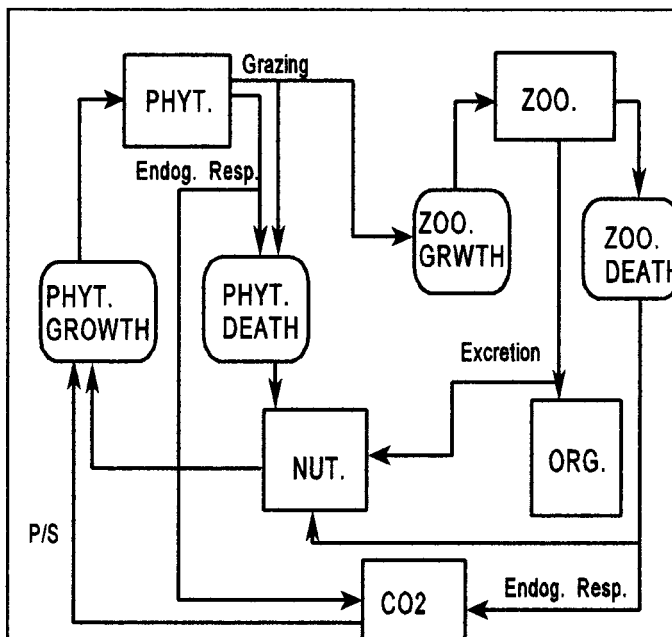
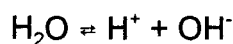
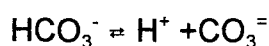
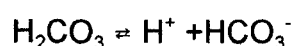
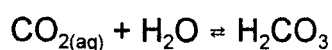


FIGURE 3: Schematic of EPCM Subsystems

Pacific system principally occur within the surface layer. Consequently, the isolation of the EPCM component activities to the surface is substantiated.

The net stocks of the five separate subsystems are determined by their inputs and outputs. The phytoplankton stock, for example, is the difference between the phytoplankton growth and death. Similarly, this has been applied to the zooplankton biomass concentration. There are three sources of nutrients within the EPCM including the death of the zooplankton, the zooplankton excretion and the phytoplankton death. However, this reserve is declined by the growth of the phytoplankton which consume nutrients in order to survive.

The carbon species within the equatorial Pacific can be broken up into two distinct categories: inorganic and organic carbon. The inorganic carbon in the atmosphere is predominantly CO₂ in the gaseous state. The initial flux, [CO_{2(g)} ⇌ CO_{2(aq)}], sets up a series of steps for carbonate equilibria as follows (*Bolin et al., 1979*):



These carbonate species are the dominate dissolved inorganic carbon species (DIC) found within the oceans (*Sarmiento, 1993*). The CO₂ pool within the EPCM has two inputs, both of similar origins. These are the result of endogenous respiration of the zooplankton and phytoplankton. Endogenous

respiration is the reverse process of photosynthesis and releases CO₂ into the immediate environment. CO₂ is released by respiration and then consumed during photosynthesis. The growth rate of autotrophic species, such as these, depends upon photosynthesis.

In addition to the inorganic carbon, organic carbon is also present within the oceanic environment. This class can be broken down into two basic subclasses which are the dissolved organic carbon (DOC) species and the particulate organic carbon (POC). DOC is produced by the dissolution of calcium carbonate found within the oceans. The POC is found in many forms, including detritus, calcium carbonate and fecal matter. The excretion products of the zooplankton are the only source of organic carbon within the simulated system since organic carbon content within the equatorial Pacific contains a large of proportion of fecal matter (*Bolin et al., 1979*).

Phytoplankton Growth Rate

The saturated growth rate of phytoplankton (**GSAT**) has been demonstrated, in a simplified manner, as being dependent upon temperature (*Di Toro et al., 1971*). This relationship is simply:

$$\mathbf{GSAT = K1 * TEMP * PHYTs} \quad \mathbf{(1)}$$

where **K1** is a constant representing the doubling of the saturated growth rate for a temperature change of 10°C, **TEMP** is the sea-surface temperature, and **PHYTs** is the phytoplankton stock of the surface layer. However, in the aquatic ecosystem, the maximum phytoplankton growth rate is limited by various factors. First, the growth of phytoplankton (**P1**) is attenuated by light, where the intensity can vary due to depth (**DPTH**) and photoperiod, *f* (ie. the daylight fraction of a day - refer to *equation 2*). Beer's Law simply states that light intensity decreases exponentially with depth. In addition, this growth term is dependent upon the extinction coefficient. A high extinction coefficient represents the existence of a great amount of particulates which attenuate the incoming solar radiation to a higher degree. This is an additive function in which the effect of suspended particles, dissolved matter, etc., is accounted for and is thus, specific to distinct water bodies (*Parsons et al., 1984*).

I₀ symbolises the light intensity at the ocean surface. Here, the incoming light is at its maximum. However, phytoplankton do not respond positively to these high amounts of sunlight. The high intensity of the solar radiation has an inhibiting affect on the phytoplankton photosynthetic rate (*Figure 4*). Thus, similar to Di Toro et al. (*1971*), the EPCM takes the average solar intensity as **I₀** at the water surface. The optimum light intensity for phytoplankton growth occurs further down the water column where the intensity is diminished. From this point, the phytoplankton growth rate progressively declines with increasing depth.

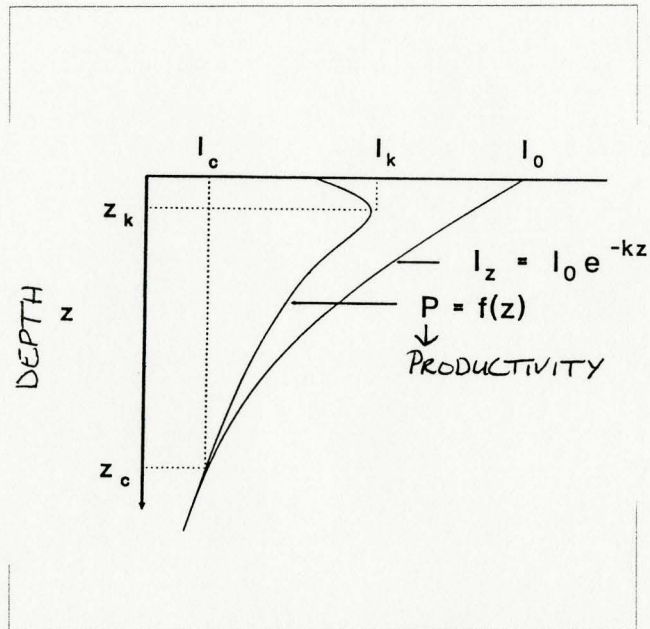


FIGURE 4 Diagram showing depth versus productivity as a function of light intensity. Productivity is inhibited at the surface and is maximum where light intensities are less.

In addition, the growth of the phytoplankton population is regulated by self-shading. As the phytoplankton concentration becomes increasingly dense, the population higher up in the water column shades those beneath them. Hence, those at a greater depth ultimately grow at slower rates since they are unable to receive maximum amounts of sun light for photosynthesis (*Valiela, 1984*).

The light limiting and self-shading term **LT** is represented in the EPCM as follows (refer to *TABLES 1 and 2* for symbol definitions and constant values):

$$LT = (2.718 * f) / (SS * DPTH) * (e^{-\alpha_1} - e^{-\alpha_0}) \quad (2)$$

where $\alpha_1 = I_0/I_s * e^{(-SS * DPTH)}$ and

$$\alpha_0 = I_0/I_s \quad \text{and}$$

$$SS = K_e + (K + (PHYTs * 1000)/Vs)$$

where **SS** defines self-shading by the phytoplankton, **K** is the extinction coefficient due to phytoplankton, **K_e** is the extinction coefficient resulting from all other attenuation factors, and **V_s** is the volume of the surface layer.

Nutrient availability is the third limitation on saturated growth of the phytoplankton. This follows the Michaelis-Menten relationship (*Equation 3*) where the phytoplankton growth increases in a first-order fashion and then reaches a luxuriant level at which growth stabilizes.

$$LIMNUT = NUT / (KM + NUT) \quad (3)$$

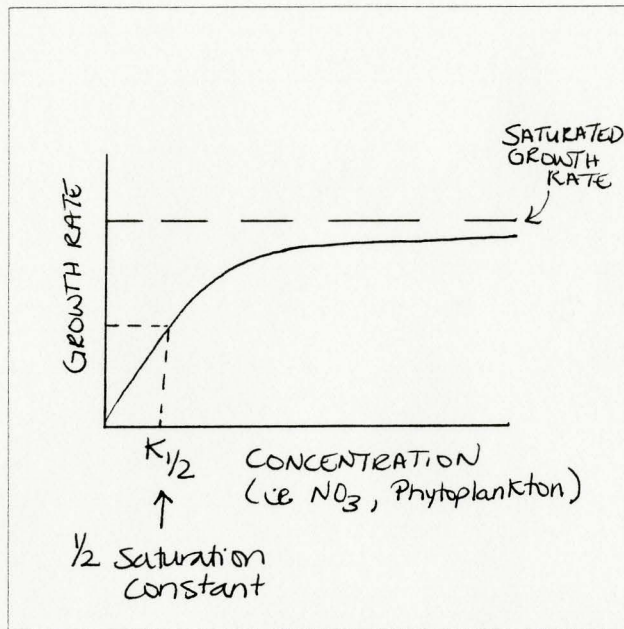


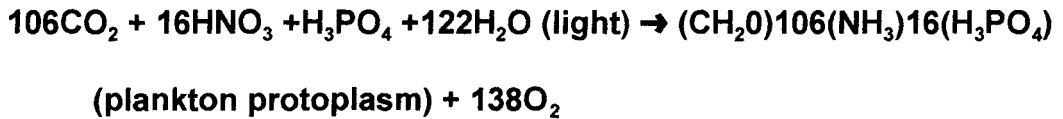
FIGURE 5: half-saturation curve

There exists, however, a point of half-saturation where a certain nutrient concentration ingested by the phytoplankton creates a growth rate that is half its maximum (*Figure 5*). Hence, the growth of the phytoplankton biomass concentration contributes to the decline of the nutrient supply within the equatorial Pacific. As previously explained, their growth depends on the availability of nutrients, as a means of subsistence, within their habitat.

Integrating all of the aforementioned terms gives the overall expression for the growth rate of the phytoplankton:

$$P1 = GSAT * LT * LIMNUT \quad (4)$$

For every unit of phytoplankton that is created, a unit of CO₂ is consumed during the process of photosynthesis. The overall reaction of the photosynthetic process in algae takes the form of (*Butcher et al., 1992*),



which is indicative of the phytoplankton - CO₂ relationship during the growth process.

Phytoplankton Death Rate

Endogenous respiration of plankton species is generally the antithesis of photosynthesis and thus, contributes to the death rates of both phytoplankton and zooplankton (see previous equation for algae photosynthesis). This has been defined as the conversion rate, by organisms, of organic carbon into inorganic carbon via oxidization per unit weight of plankton carbon (*Di Toro et al., 1971*) and is represented in the model as,

$$P2 = K2 * TEMP * PHYTs \quad (5)$$

where **P2** represents the death rate of the phytoplankton via endogenous respiration and **K2** is the endogenous respiration constant for phytoplankton.

During the process, the plankton release CO₂ into their surrounding environment, contributing to the inorganic carbon pool within the equatorial

Pacific. This mechanism has been shown by Riley et al., (1949 from Di Toro et al., 1971) to be positively dependent upon sea-surface temperature such that, as the temperature rises the rate of respiration increases as well (Di Toro et al., 1971). The linear relationship is a simplification of the natural mechanism, and is used as an approximation in the EPCM. Similar to the photosynthetic relationship between phytoplankton growth and CO₂, the reduction of one unit of phytoplankton biomass from endogenous respiration creates one unit of CO₂. The respiration process follows the same reaction as the photosynthesis process, but in the reverse direction.

The death of the phytoplankton, due to respiration, also releases nutrients into its surrounding environment. The nitrogen content of the phytoplankton exist in an approximate ratio of 108:15 (=C:N) with carbon (Butcher et al., 1992) which is in accord with the observations made by Redfield (Fielder et al., 1991).

The second mode of phytoplankton death described by the EPCM is due to the grazing action of the predaceous zooplankton within the system (Equation 6). The maximum death rate of the phytoplankton due to predation by zooplankton is simply a function of the zooplankton filtering rate and their population size. However, the amount of phytoplankton grazed is restricted by the available phytoplankton for consumption. This is comparable to the limitation on phytoplankton growth by nutrient availability such that it also follows the Michaelis-Menten trend (see Equation 3).

Zooplankton Growth Rate

As the zooplankton grazing rate decreases the phytoplankton stock, it simultaneously contributes to the zooplankton growth rate (**P3**) in the same manner. The basic equation for the single process follows the proceeding form:

$$P3 = (CG * ZOOs * PHYTs * (PHYTs / (KMP + PHYTs))) / Vs \quad (6)$$

where the product of the filtering rate (**CG**) per unit biomass of the zooplankton present within the surface layer (**ZOOs**) and the phytoplankton biomass concentration symbolizes the zooplankton grazing rate, having units of day⁻¹. Zooplankton may be represented fairly accurately by the actions of the microzooplankton alone. This is due to the fact that mesozooplankton rarely consume more than a small fraction of daily primary productivity (ie. less than 20%) (*Longhurst, 1991*). For this reason, the grazing rate of the zooplankton is taken as that of the microzooplankton, as determined by Murray et al. (*1994*).

However, the zooplankton has a limitation on its ability to grow. As with the phytoplankton growth rate and the limiting nutrient, the zooplankton's growth is regulated by the availability of phytoplankton within the area. A half-saturation constant (**KMP**) is once again incorporated into the growth term of the zooplankton in order for the uptake of phytoplankton to follow Michaelis-Menten kinetics.

Zooplankton Death Rate

As with the phytoplankton, the zooplankton's death (**P4**) is due to endogenous respiration. This is delineated within the EPCM as:

$$P4 = K3 * TEMP * ZOOS \quad (7)$$

Again, this is a linear function utilizing an endogenous respiration constant specific to zooplankton (**K3**), where death correlates positively with increasing temperature. Furthermore, the respiration adds to the inorganic carbon content of the ocean, since respiration requires that CO₂ be emitted from the zooplankton system.

In addition, the zooplankton biomass consists of a carbon-to-nitrogen ratio of 103:16.5 (*Butcher, 1992*). Thus, the death of zooplankton contributes to the nutrient reservoir of the equatorial Pacific.

Zooplankton Excretion Rate

The fecal matter of zooplankton accounts for 98% and 95% of the total particle volume in the upper 100 m and deeper waters, respectively (*Bishop et al., 1980*) in areas having similar qualities as the equatorial Pacific. Since the zooplankton excretion (which is classified as particulate organic carbon or POC) represents one of the most significant contributors to the organic carbon pool of the equatorial Pacific, the excretion rate is the only process of the EPCM which

adds to the organic carbon concentration of the system. For every unit of the zooplankton carbon concentration lost to the excretory process, a unit of organic carbon is released.

In addition to contributing to the organic carbon concentration, the fecal pellets contain a certain percentage of nutrients (ie.nitrogen), as well. The amount of carbon created in this process is simply converted to its corresponding nutrient amount.

The actual process rate for the excretion of zooplankton takes on the following form within the EPCM:

$$P5 = (CG * ZOOs * PHYTs * (1 - (PHYTs / (KMP + PHYTs)))) / Vs \quad (8)$$

Equation 8 can be translated as the difference between the rate that phytoplankton are ingested and the rate of metabolism. Hence, the consumed phytoplankton are assumed to take only two pathways within this system. After ingestion, the zooplankton food may become metabolised and utilized as an energy source for everyday activities. However, some of the consumed carbon may simply be disposed of through excretion.

(3) TRANSFER MECHANISMS

As previously discussed, the transfer mechanisms within the equatorial Pacific are significant parameters in the comprehension of the fate of carbon species throughout this area. The physical processes are the primary contributors to the carbon fluxes within this region since they control much of the low-frequency biological and chemical variability (Murray *et al.*, 1994). The incorporation of the physical dynamics of the system allows for the determination

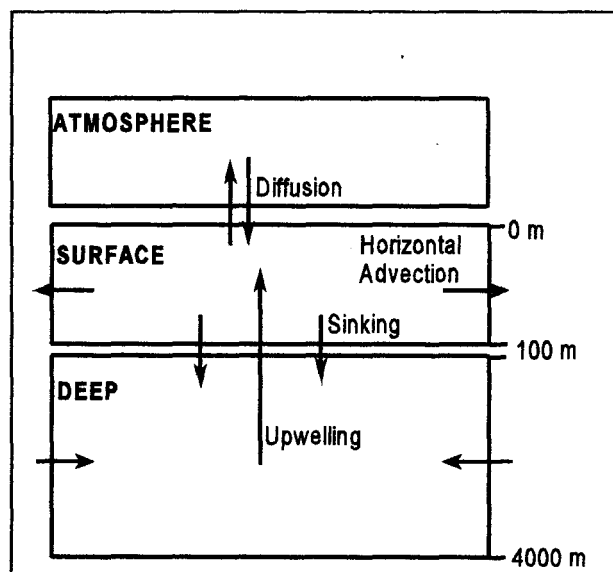


FIGURE 6 - Transfer mechanisms of the EPCM

of mass balances. Conservation of mass is an important concept to keep in focus while modelling any natural system. This basically keeps the considered substances accounted for by mass transport into or out of the volumetric segment being observed or as mass is being produced or consumed within that same

segment (*Di Toro et al., 1971*) For instance, new production is estimated as the net input of nitrate into the productive zone by horizontal and vertical advection (*Fielder et al., 1991*) Within the EPCM, transport of substances is recognized on a horizontal and vertical scale (*Figure 6*)

Horizontal Advection - The Equatorial Current

The circulation of the water masses in the upper layers of the tropical Pacific is dominated by the North and South Equatorial Currents (*Figure 7 from Fielder and Philbrick, 1991*) The strength and direction of these currents are highly sensitive to the wind system and subsequently show seasonal variations (*Neumann, 1968*). The South Equatorial Current (SEC) provides the outflow from the surface compartment. This current is westward in direction and is influenced

mainly by the easterly trade winds travelling in a westward direction parallel to the equator The Coriolis force, created by the rotation of the Earth, causes movement of a particle on the Earth's surface to be accelerated at right angles to the line of motion Hence, the SEC and the North Equatorial Current (NEC)

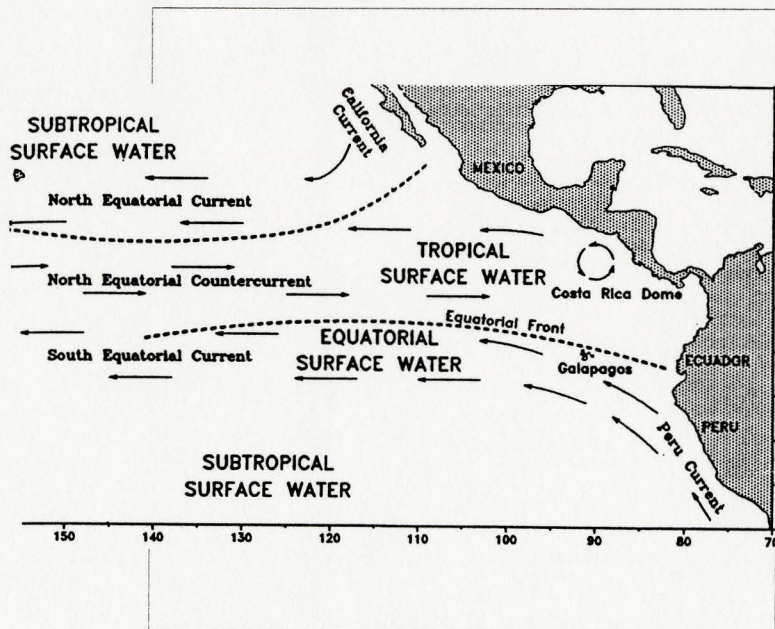


FIGURE 7: Currents of the Equatorial Pacific

diverge away from the equator and veers to higher latitudes (*Figure 8*). In this way the surface water is moved out and away from the tropical Pacific area (*Thurman, 1991*)

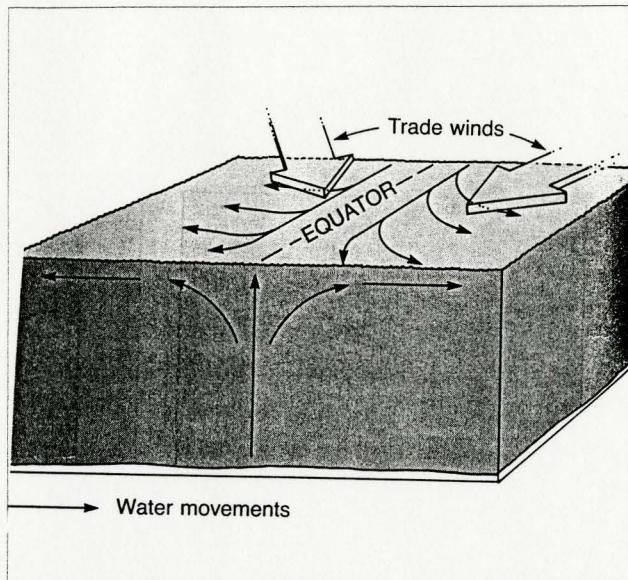


Figure 8. Upwelling Process in the Open Equatorial Pacific Ocean

The Equatorial Undercurrent (EUC) travels eastwards beneath the surface layer at approximately the depth of the thermocline (*Philander et al., 1987*) The thermocline is a region located below the mixed or surface layer in which temperatures are rapidly changing Thermocline, typical of tropical oceans, tend to be deeper and more permanent than

those at higher latitudes (*Knauss, 1978*). Since the EPCM does not actually include a thermocline, the EUC has been designated as being part of the deep layer The movement of the EUC supplies component substances to the subsurface layer

The horizontal rate of inflow (**EUCX**) of the principal species into the deep layer compartment is represented within the EPCM as the product of the inflow of water due to the EUC (**Qin**) and the concentration of the species entering with that current (**Xin**).

$$\text{EUCX} = \text{Qin} * \text{Xin} \quad (9)$$

Here, X signifies the substance of interest (eg. PHYT, ZOO, etc.)

The same idea is utilized for the outflow of substance concentration by way of the South Equatorial Current, or SEC. However, the corresponding concentration exiting the surface layer replaces the input concentration.

The rate of horizontal transport out of the surface layer, **OUTX**, occurs by way of the South Equatorial Current, or the SEC. The amount of component lost via horizontal advection corresponds to the stock of the substance in the surface layer (**Xs**). This is taken as the product of the rate of outflow (**Qout**) and the stock taken as a concentration (simply by dividing the stock in grams by the surface volume, **Vs**):

$$\text{OUTX} = \text{Qout} * (\text{Xs}/\text{Vs}) \quad (10)$$

Upwelling

The equatorial Pacific is identified as one area of intense upwelling and uniquely distinguishes this region from other oceanic areas. Upwelling is the most important transport process in the EPCM. It is the mechanism by which deep water is brought to the surface, subsequently connecting the horizontal advective terms. It is in this way that the Equatorial Undercurrent (EUC) water is

transferred to the surface layer. This vertical mass transport occurs whenever there is a divergent flow of surface water. Since continuity requires that the depleted water be replaced, the water loss due to the divergence is recovered by upwelling cold waters from the deep layer of the ocean. The source of the upwelled water is rich in nutrients and CO₂, thus, accounting for the high primary productivity of the surficial region of the equatorial Pacific.

The upwelling mechanism of the EPCM incorporates the velocity of the upwelling motion (**vWup**). The overall term for the upwelling rate (**WupX**), for a specific substance X, is defined as,

$$\mathbf{WupX} = (\mathbf{vWup} * \mathbf{A} * \mathbf{Xdeep}) / \mathbf{Vs} \quad (11)$$

where **A** is the area of the study region and **Xdeep** represents the component stock of the deep compartment.

Downwelling or Sinking

Equatorial upwelling is balanced by adjacent downwellings in the tropics. Downwelling is the reverse vertical flux of upwelling. Previous models of equatorial circulation have included downwelling terms which penetrate into the thermocline in such a way that the circulation involves tropical subduction (*McCreary, 1981; McPhaden, 1981 - from McCreary and Lu, 1994*). The EPCM joins the subducted flow to the EUC, which completes the circulatory path in a

closed loop. The downwelling or sinking rate is, however, small in comparison to the upwelling rate. Since the upwelling rate is so large relative to the downwelling rate, there is an accumulation of materials (ie. CO₂) in the surface layer. In addition, this vertical downwards motion accounts for the sinking of fecal pellets and decline in phytoplankton concentration at the surface. Being non-motile species, the phytoplankton cannot resist the downward flux, which, consequently reduces their productive population size (*Di Toro et al., 1971*).

The downwelling term (ie. **WdownX**, which is the downwelling rate for the component X) represented in the EPCM is similar to that for upwelling. It incorporates the mean downward velocity (**vWdown**) of the surface area and the transferring of the surface stock of substance X (**Xs**) to the deep layer.

$$\mathbf{WdownX} = (\mathbf{vWdown} * \mathbf{A} * \mathbf{Xs}) / \mathbf{Vs} \quad (12)$$

Movement Between the Surface and the Atmospheric Layer

The exchange of CO₂ across the ocean-atmosphere boundary is diffusion dependent. The surface layer and the atmosphere, after some time period, reach a point of equilibration with respect to the CO₂ concentration within each of the two compartments. The EPCM assumes an equilibrium concentration [**H₂CO₃eq**] within the surface layer in accordance to Henry' Law, incorporating the partial

pressure of CO₂ (**pCO₂**) in the atmosphere. It is also assumed that this pCO₂ changes negligibly.

Henry's Law is the theory that is utilized for the atmospheric - surface layer transfer. Generally, it states that the vapour pressure of a volatile solute (B) is proportional to its mole fraction in a solution (**X_B**), where **H_B** is the constant characteristic of the solute (ie. Henry's constant - *Atkins, 1993*):

$$pB = X_B * H_B \quad (13)$$

Accordingly, the Henry's constant utilized in the EPCM, specific for 25°C and 19% chlorinity (or Cl), is 10^{-1.53} mol/l/atm (*Stumm and Morgan, 1970*).

The equilibrium reaction for the dissolution of gaseous CO₂ into water is,



and leads to the formation of H₂CO₃ within the surface waters. Total dissolved carbon in the surface compartment (**CO_{2s}**) for the EPCM is represented by the sum of the carbonate species found within oceanic waters:

$$CO_{2s} = [H_2CO_3] + [HCO_3^-] + [CO_3^{2-}] \quad (15)$$

The changes in the H_2CO_3 levels within the surface layer changes with variations in sea-surface temperatures. Alkalinity, as well as the correction term for borate is assumed to remain constant in the EPCM conditions. Therefore, the acidity of the surface waters is defined by the term,

$$[H^+] = [H_2CO_3^{eq}] / K'_1 * ALK \quad (16)$$

where K'_1 is the first acidity constant and **ALK** is the alkalinity of the surface waters corrected for a constant borate concentration. This term is related to the non-equilibrium H_2CO_3 concentration found in the surface waters, by the following relationship:

$$H_2CO_3^t = CO_2s K'_1 / [H^+] + K'_1 \quad (17)$$

Hence, the increases in the non-equilibrium H_2CO_3 value change as the total CO_2 (**CO2s**) concentration within the surface layer changes.

The determination of the actual flux between the surface layer and the atmosphere calculates the difference between the equilibrium concentration of H_2CO_3 and the non-equilibrium H_2CO_3 concentration in the surface water. Finally, the ocean-atmosphere flux, **Fsa**, may be defined as follows:

$$Fsa = HC * (D/A) \quad (18)$$

where HC is the change in H_2CO_3 and D is the diffusion coefficient for the ocean-atmosphere gradient, controlling the rate of exchange. A positive value indicates that the surface concentration exceeds the equilibrium CO_2 concentration and is, thus, released to the atmosphere. A negative value denotes net movement of CO_2 towards the ocean and a value equivalent to H_2CO_{3eq} represents a flux of 0 magnitude.

Movement Between the Atmospheric Layer and the Earth's Atmosphere

A separate box was added on to the atmospheric compartment representing the remainder of the Earth's atmosphere and its corresponding mean CO_2 concentrations. As previously mentioned, it is necessary to include this box in order to keep the atmospheric compartment CO_2 concentrations at a reasonable level. It allows the accumulating CO_2 to move into or out of the atmospheric layer by Fickian mechanics.

$$F_{ae} = (HD * ((co2econc/1000) - (CO2atm/Vatm))/Ax) * Vatm \quad (19)$$

Since the movement here is in the horizontal direction, the flux out of or into the local atmosphere (F_{ae}) is over the cross-sectional area of the two atmospheres, A_x . HD is the horizontal diffusivity coefficient (*Bolin, 1981*), acting in a similar fashion as D . It controls the magnitude of the concentration within the atmospheric layer. For example, a large transfer coefficient, maintains a smaller

concentration of CO₂ within the local atmospheric layer and allows quicker migration of CO₂ into the Earth's atmosphere. Again, a concentration difference is taken. However, the difference taken is with respect to the local atmosphere concentration of CO₂ and that found within the rest of the Earth's atmosphere (**co2econc**).

Similar to the ocean-atmosphere flux, it is possible to determine the direction of movement by sign designation. If the concentration in the Earth's atmosphere has a negative value that exemplifies the fact that the CO₂ concentration within the atmospheric layer is large, CO₂ will move out of that compartment and into the Earth's compartment. However, if the value is positive, then the CO₂ direction of movement is from the Earth's atmosphere and into the atmospheric compartment of the equatorial Pacific.

(4) THE PETERSON'S MATRIX AND THE INTEGRATION OF PROCESSES

General Introduction to the Peterson's Matrix

Comprehension of how each of the components and processes of a model interact, is clearly seen in a matrix format. This method of model presentation is often referred to as the Peterson's Matrix (*Peterson, 1965*). It is a matrix often used in the study of wastewater treatment problems. There are basically four elements comprising the matrix itself: the components of the model, the processes occurring in the system which affect each of the components, the kinetic parameters utilized within the corresponding kinetic or rate expressions, and the stoichiometric coefficients which set out the mass relationships between the components in the individual processes.

Peterson's Matrix With Respect to the EPCM

Accordingly, the EPCM was formatted into a similar layout (*Figure 9*). The components (ie. phytoplankton, zooplankton, nutrients, carbon dioxide and organic carbon) of the EPCM are located at the top of the matrix and their complete titles are found at the bottom of the matrix in the corresponding column. The processes are listed down the far left-hand side and their rate terms are defined in the rightmost column of the matrix, with the definitions of each of the kinetic parameters directly below. The core of the matrix describes how the components are related to one another with respect to mass. It is also within the core of the matrix where the stoichiometric coefficients come into effect. To

PETERSON'S MATRIX FOR EPCM

FIGURE 9

COMPONENT (i)	(1) PHYT	(2) ZOO	(3) NUT	(4) CO2	(5) ORG	PROCESS RATE [gC/day]
PROCESS (j)						
PHYT. GROWTH	+1		-U	-1		$(K1 * TEMP * PHYTs) * ((2.718^{f/SS * DPTH}) * (EXP(-(I_0/Is)) * EXP(-(SS * DPTH))) - (EXP(-(I_0/Is)))) * (NUTs / (KM + NUTs))$
PHYT. DEATH (ENDOG. RESPIRATION)	-1		+U	+1		$K2 * TEMP * PHYTs$
ZOO. GROWTH (GRAZING)	-1/Y	+1				$((CG * ZOOs * PHYTs) * (PHYTs / (KMP + PHYTs))) / Vs$
ZOO DEATH		-1	+Z	+1		$K3 * TEMP * ZOOs$
ZOO. EXCRETION RATE		-1	+Z		+1	$((CG * ZOOs * PHYTs) * (1 - (PHYTs / (KMP + PHYTs)))) / Vs$
Reaction Term (Ri)	$R_i = \sum v_{ij} * P_j$					
Stoichiometric Parameters: utilization efficiency: Y nutrient to phyto. biomass conc. U nutrient to zoo. biomass conc.. Z	Phytoplankton Stock [gC]	Zooplankton Stock [gC]	Limiting Nutrient Stock [gNO3]	Total CO2 (inorganic carbon) Stock [gC]	Organic Carbon Stock [gC]	Kinetic Parameters: Doubling of saturated growth rate: K1 self-shading effect: SS half-sat'n constant for phyt. growth: KM phyt. endogenous respiration constant: K2 filtering rate for zooplankton: CG half-saturation constant for zoo. growth: KMP zoo. endogenous respiration constant: K3

exemplify how this layout functions, the zooplankton growth due to grazing is described. The matrix explicitly describes how the phytoplankton and zooplankton are related by mass. One unit of zooplankton that grows from the grazing action corresponds to a loss of $1/Y$ units of phytoplankton due to the grazing of zooplankton.

Another way in which the Peterson's Matrix is useful to the modeller is for the verification of continuity, simply by inspection. By moving across the core of the matrix, and provided that consistent units have been used, the sum of the stoichiometric parameters found must be equal to zero. This is equivalent to the idea of mass conservation. Thus, in the EPCM it can be seen that continuity has, in fact, been obeyed. This may not be obvious at a glance when observing all five component columns. However, the units for the nutrients (gNO_3) are different from the other components and are, therefore, not taken into consideration when checking for constancy.

Reaction Rates

As previously mentioned, it is pertinent that conservation of mass is applied when modelling this type of system. Generally, mass balance may be equated for any system by the following term:

$$\text{INPUT} - \text{OUTPUT} + \text{REACTION RATE} = \text{ACCUMULATION} \quad (15)$$

The reaction rate may easily be calculated by summing the products of the stoichiometric coefficients and the process rate expressions for each of the components being considered in the mass balance.

$$R_i = \sum v_{ij} * P_j \quad (16)$$

For instance, in the EPCM the reaction rate for the phytoplankton is basically the difference between the phytoplankton growth rate and death rates. Symbolically, this term would be as follows:

$$R1 = P1 - P2 - (P3 / Y) \quad (17)$$

where **R1** is the reaction term for the component of phytoplankton, **P1** is the phytoplankton growth process rate, **P2** is the process rate for the phytoplankton death due to endogenous respiration, and **P3** is the process rate for the phytoplankton via zooplankton grazing. This term is then utilized within the mass balance reaction for phytoplankton accumulation in a selected compartment.

Mass Balances

With a comprehension of the reaction terms it is simple to construct mass balance equations for each of the layers. All that is required are the fluxes for each of the transfer processes. As mentioned in the previous section, for each

layer the rate of substance accumulation is simply the rate of input minus the rate of output added to the reaction rate. For example, the surface layer, with respect to the phytoplankton stock (**PHYTs**), has an input from upwelling (**Wup1**) and two outputs via downwelling (**Wdown1**) and horizontal advection out of the surface compartment (**OUT1**) (**Figure 6**). So, in this case the mass balance term would simply be:

$$\text{PHYTs} = \text{Wup1} - (\text{Wdown1} + \text{OUT1}) + \text{R1} \quad (18)$$

Hence, the mass balance term integrates all of the processes and components into a single system, where the magnitudes of each of the components affect the others and the compartments are linked together.

(5) DESCRIPTION OF MODEL RUNS AND RESULTS

Steady-State

To determine the steady-state values for the EPCM, a standard run using the original initial values (*Table 2*) was performed. The data that was utilized in the study was a result of the Joint Global Ocean Flux Study (JGOFS). The values were averaged over the entire study area and divided between the surface layer (ie. 0 to 100m) and the deep layer (ie. greater than 100 m). The simulation was run for more than a 100 year period, having a time-step of a seasonal basis. The results for the simulations, in acquiring steady-state times, are shown in

Figures 10a to 10e. The graphs represent the progression of each of the five component concentrations in the deep and surface layers with time. Steady-state is initially reached at different times for each; however, by approximately 70 days into the run all of the concentrations are sufficiently stable. Some of the other resulting plots do show changes after this time, but the differences are small and probably insignificant (ie. less than a thousandth of a change) The steady-state concentrations obtained in this run (*Table 3*) are used in all of the other tests as the new initial values.

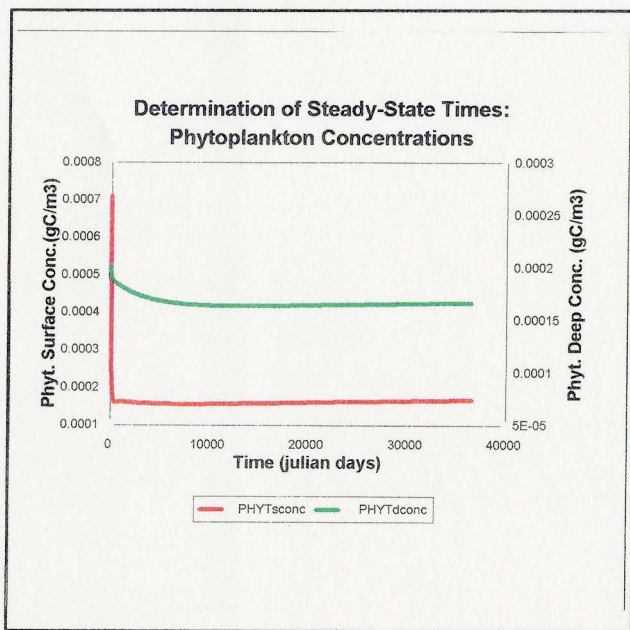


FIGURE 10a

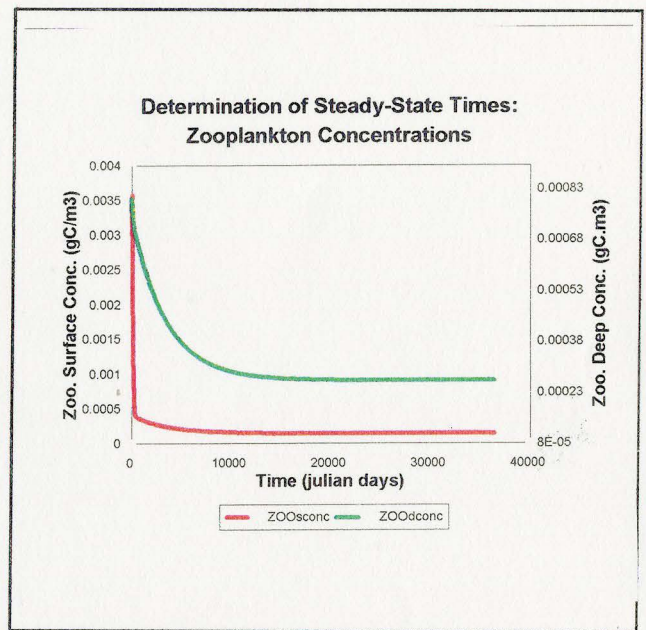


FIGURE 10d

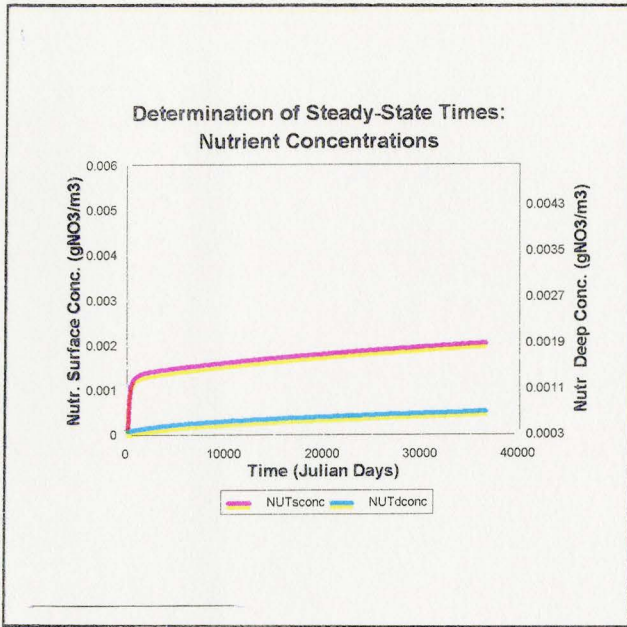


FIGURE 10c

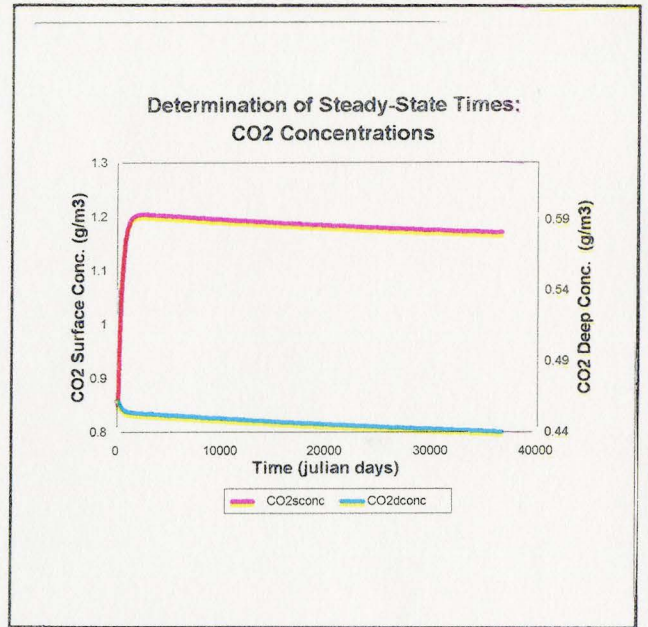


FIGURE 10b

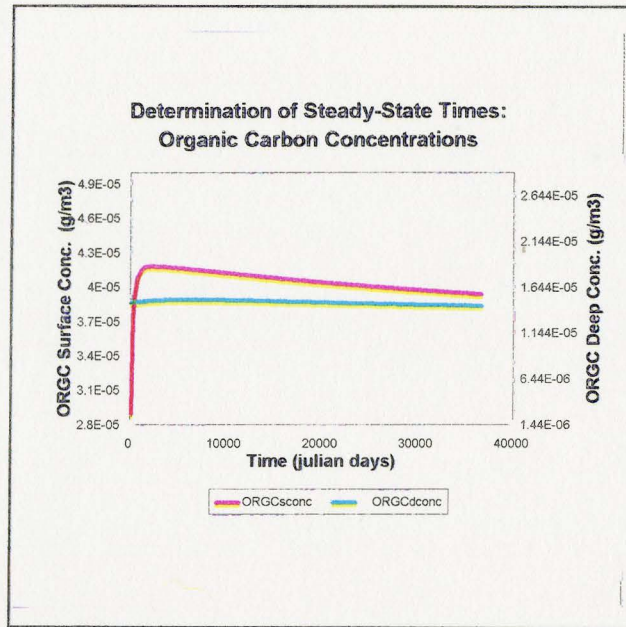


FIGURE 10e

SENSITIVITY ANALYSIS

The process rates, upwelling and component concentrations were all analyzed to determine the effects of different environmental conditions. Each model run spanned 86 years beginning in January 1900 and had a time step of one hundred days. The period of one hundred days incorporates the most significant seasonal changes. The model also included a data file which executed values for the concentration of CO₂ in the entire Earth's atmosphere (**CO2econc**) over time. The incorporation of this data file allows for major changes in atmospheric carbon (particularly CO₂) to be considered as an external force. For instance, the 1900 to 1986 period represents changes due to the industrial revolution and short-term climatic changes, in particular, El Niño events. Two different environmental variables that directly interact with the system parameters were considered in the sensitivity analysis. These include sea-surface temperature (SST) and upwelling velocity. It is important to look at these two variables in this study since the principal focus of the study is to examine the effect that climatic anomalies, such as the El Niño, have on atmospheric CO₂ levels.

El Niño

The dynamic distribution of carbon within the equatorial Pacific has, in the past, been upset by a short-term climatic event known as the El Niño. This

complex condition is somewhat periodic in nature, but does not occur at regular intervals. The approximate frequency, however, is about one event every two to ten years (*Carrquiry et al., 1994*) persisting for six to 18 months (*Barber and Chavez, 1983*). Generally, anomalously high temperatures and precipitation levels are encountered in specific regions over the equatorial Pacific. West of the dateline the conditions seem to be dominated by high rainfall patterns whereas, in the study region (east of the dateline) high temperatures are the forcing condition during these periods of change (*Cole and Fairbanks, 1990*).

Often the El Niño is referred to as the El Niño/Southern Oscillation or ENSO. The Southern Oscillation accompanies the El Niño and is an immense seesawing of atmospheric pressure between the southeastern and the western tropical Pacific (*Ramage, 1986*). During El Niño periods a higher than normal difference between sea level pressures of the two regions is evident (*Cole and Fairbanks, 1990; Ramage, 1986*).

Thus, it may be inferred from the previous section that the ENSO event results in a coupled ocean-atmosphere interaction creating characteristic changes in both of these mediums. One of the more predominant results of the El Niño in the eastern equatorial Pacific is a rise in sea-surface temperature. Normal sea-surface temperatures are unusually cool in the eastern region of the equatorial Pacific. Basically, this is due to the intense upwelling action of this region which transports deep, cool waters from below the thermocline to the surface. However, the typically strong upwelling process weakens during El Niño

events. Surface waters thus, receive much less cool water to dissipate the solar radiation being input into the Pacific. The weakening of the upwelling rate is another significant change that accompanies EN/SO events. The divergence of surface water, which creates the upwelling motion, is caused by a combination of the easterly trade winds and the Coriolis force. The trade winds force the surface water in a westerly direction parallel to the equator. However, the motion of the Earth creates an apparent force (ie. the Coriolis force) causing the water to accelerate at right angles to the line of the original motion. In effect, the surface waters on either side of the equator move to higher latitudes (*Thurmann, 1991*). It has, in fact, been observed that the weakening of the south Pacific high pressure during El Niño periods is accompanied by a significant decrease in surface wind strength, therefore, causing upwelling to become less intense and increasing sea-surface temperatures (*Diaz and Kiladis, 1992; Ramage, 1986*).

The weakening of the upwelling motion subsequently decreases nutrient uptake from the deep. Phytoplankton depend on nutrient intake for growth and survival thus, the decrease in nutrient concentration causes a large decline in productivity within the surface layer. There is a commensurate uptake of carbon during primary production in the ratio of carbon:nitrogen:phosphorus of 106:16:1. With a decrease in phytoplankton growth and stock, the carbon circulation within the equatorial Pacific slows, reducing the carbon pools to a further extent. Other processes, such as atmosphere-ocean CO₂ equilibration, are affected by temperature changes. As previously mentioned, it has been remarked that the

equatorial Pacific actually acts as a net sink for CO₂ during these anomalous, El Niño events.

Temperature Effects

Four different temperatures were compared in these simulations to determine how each process rate and component concentration reacts to changing sea-surface temperatures. 26.7°C is the average temperature for the equatorial Pacific region according to the compiled mean monthly average SST data file (NOAA - FERRET DATABASE). 29.5°C represents the approximate maximum SST for the 86-year period. This is indicative of El Niño and thus, using this value enables observations of one of the anomalous parameter changes viewed during these events. 25.2°C is the lowest measurement of the SST record used in the EPCM. However, a value of 24°C (10% less than the average SST) is also analyzed in order to compare the 29.5°C SST, which is 10% greater than the average temperature.

● Phytoplankton

The concentrations of phytoplankton that the model simulated were comparable to those that were observed in the field (Murray *et al.*, 1994) at an approximate range of 10⁻³ to 10⁻⁴ g/m³.

Figure 11a shows that the average SST is the optimum temperature for phytoplankton growth rates. It is also evident that growth rates are limited by

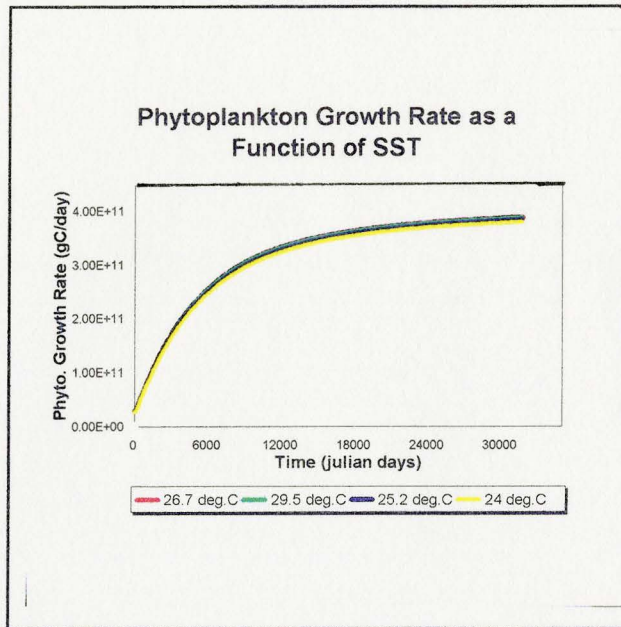


FIGURE 11a

higher and lower temperatures than the average with the colder temperatures having a greater effect on phytoplankton growth than do warmer temperatures. Exemplifying this is the fact that the maximum temperature run presents a growth rate difference from the average of an order of magnitude of 10^9 gC/day or less, whereas the difference between the average and the 24°C run was close to 2×10^{10} gC/day. Overall, however, a 2×10^{10} gC/day change in rate is not large. The difference between the minimum temperature and the average is fairly small at approximately 5%.

Phytoplankton death rate as a function of temperature exhibits a very similar pattern to that of the phytoplankton growth rate in magnitude and in form (Figure 11b). However, the upwelling rate for phytoplankton contrasts the death and growth rates in such a way that the cooler temperatures tend to raise the

upwelling rate (Figure 11c) The largest change from the average results from the 24°C run In magnitude this is equivalent to a difference of approximately 2×10^9 gC/day, but again the percentage change is rather small (~3.6%)

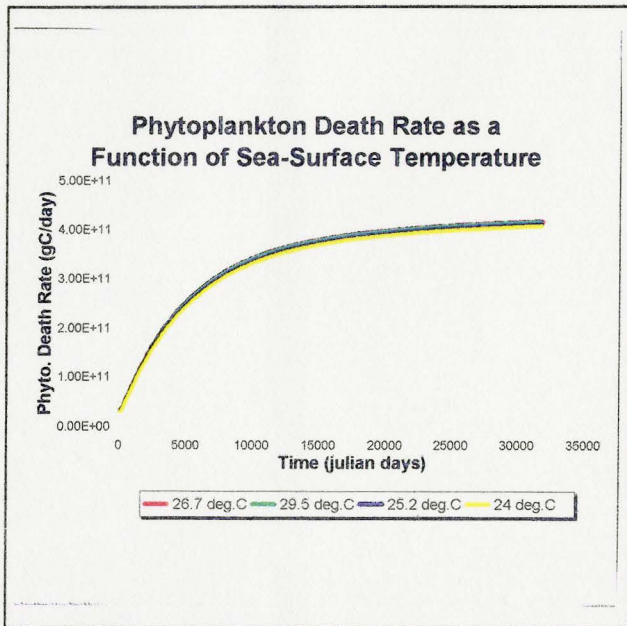


FIGURE 11b

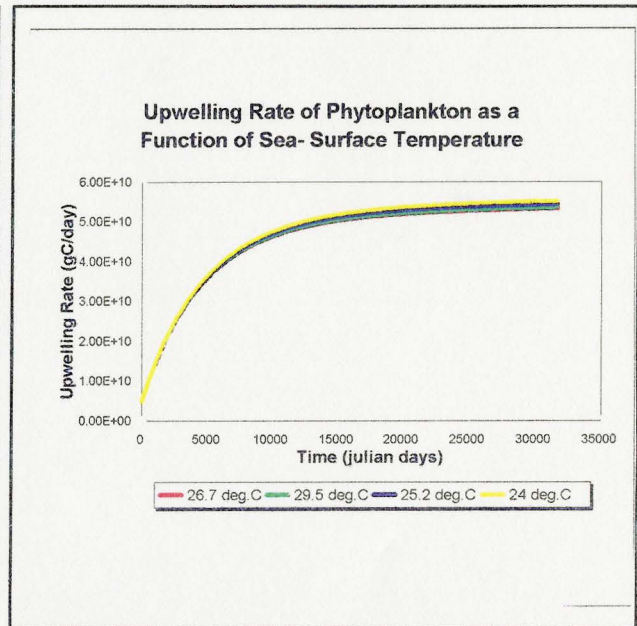


FIGURE 11c

Figure 11d shows the effect of temperature on the actual phytoplankton concentrations. In 1986, the concentrations decrease with increasing SST, although the effect of SST on phytoplankton concentrations within the deep layer is less than the effect on the concentrations in the surface layer In the deep layer, the percentage change from the norm is approximately 4 - 4.5%, for both the minimum and maximum, by a difference of about 8%. In each instance the effect of the actual minimum temperature (25.2°C) creates an effect about half that of the 24°C temperature. This follows the results observed previously, where periods of El Niño and its corresponding high temperatures had and has

the effect of reducing primary productivity (*Barber and Chavez, 1983; Murray et al., 1994, Ramage, 1983*)

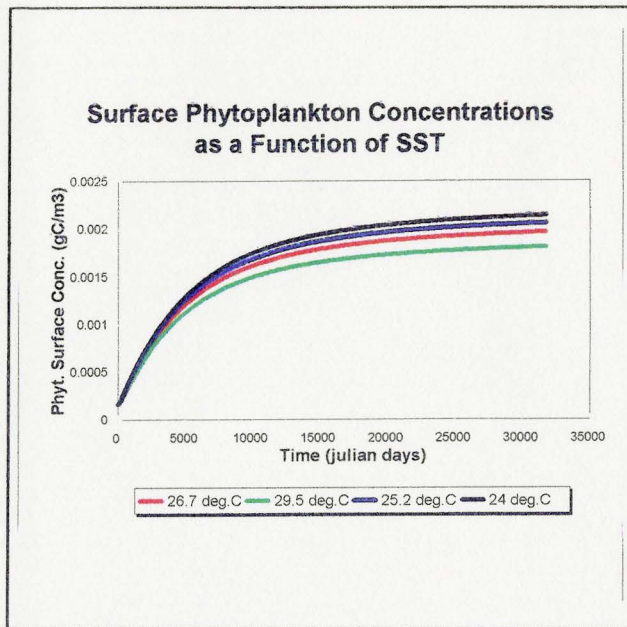


FIGURE 11d

- Zooplankton

Figure 12a suggests that zooplankton are insensitive to temperature changes. However, observance of the zooplankton death rate as a function of sea-surface temperature (*Figure 12b*) displays that the influence of colder temperatures has a positive correlation with their death rate. Both *figures 12a and 12b* suggest that according to the EPCM the zooplankton prefer a warmer environment than one that is cool (ie. less than 26.7°C)

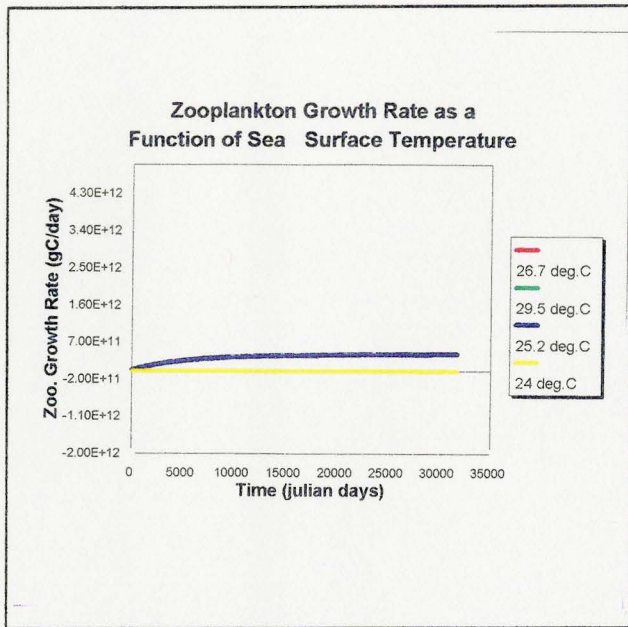


FIGURE 12a

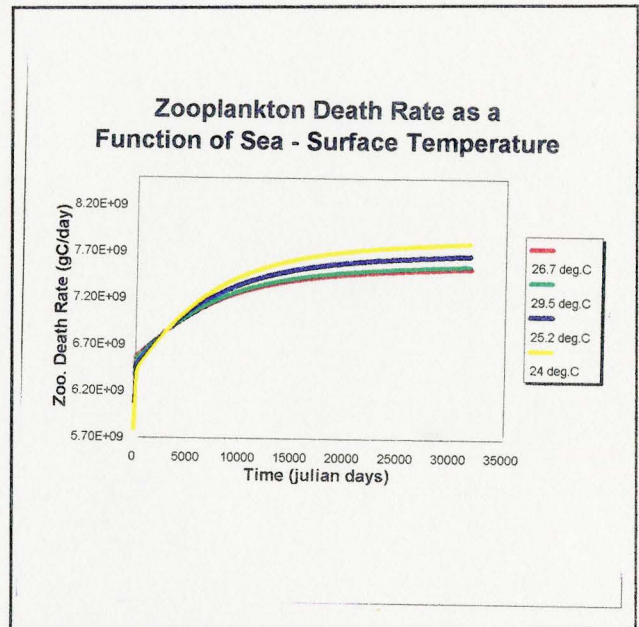


FIGURE 12B

With the EPCM, it was also determined that the transfer of the zooplankton from the deep to the surface waters is inversely proportional to temperature (*Figure 12c*). In other words, upwelling rate increases with decreasing temperature. This is concurrent with the fact that the upwelling function of the EPCM is dependent upon the zooplankton concentration of the oceanic deep compartment (*Equation 11*). At temperatures less than the average, the upwelling rate changes according to the concentration variations within the deep layer, which increase with decreasing SST. Similarly, the surface layer responds with direct proportionality to temperature.

Whereas the upwelling rate is not very sensitive to changes in temperature ($\leq 3\%$ changes from the average), the zooplankton concentrations are affected by temperature change. This suggests that zooplankton concentrations are

sensitive to small changes in upwelling intensity; surface zooplankton concentration (*Figure 12d*) changes of 15% correspond to a 3% change in upwelling. Thus, the response of upwelling to a minimum temperature value may seem insignificant, but in actuality that is not the case. The sensitivity of zooplankton concentrations to fluctuations in upwelling demonstrates that upwelling is an important parameter with respect to the cycling of carbon

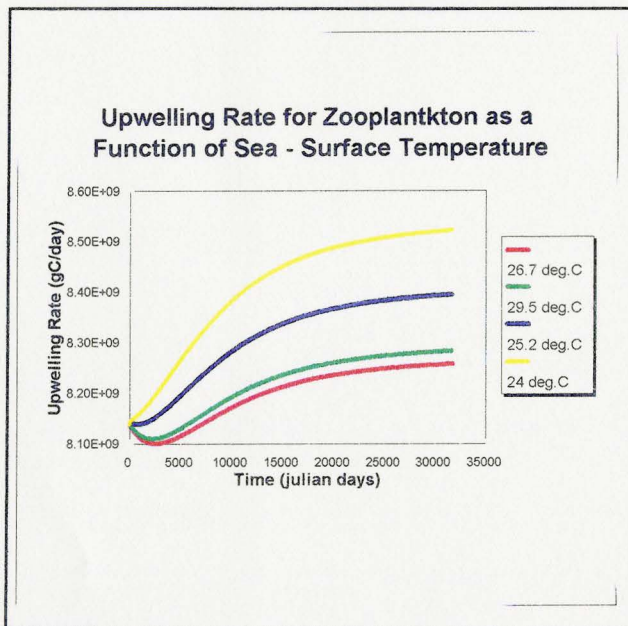


FIGURE 12c

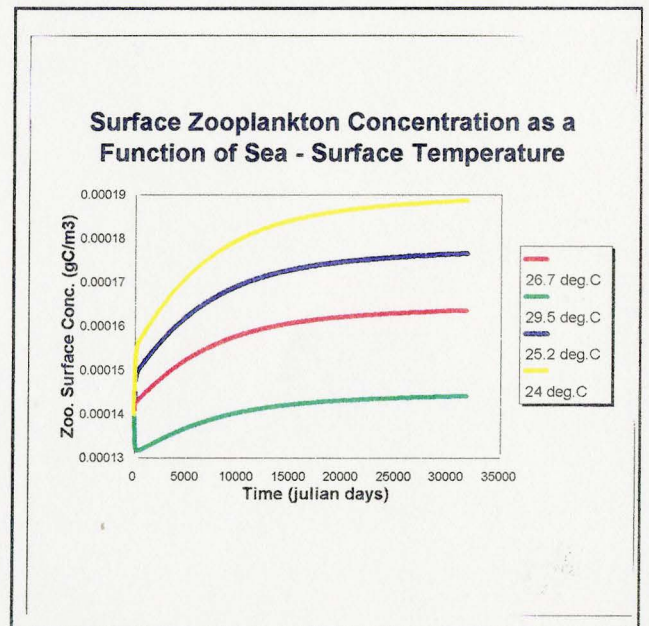


FIGURE 12d

- **Nutrients**

In the EPCM, nutrients cycle among phytoplankton, zooplankton death products, and fecal matter of zooplankton. The graphs shown in *figures 13a and 13b* emphasize the unresponsive nature of nutrient transfer and concentration to temperature variations. Also indicated in these graphs is that nutrient

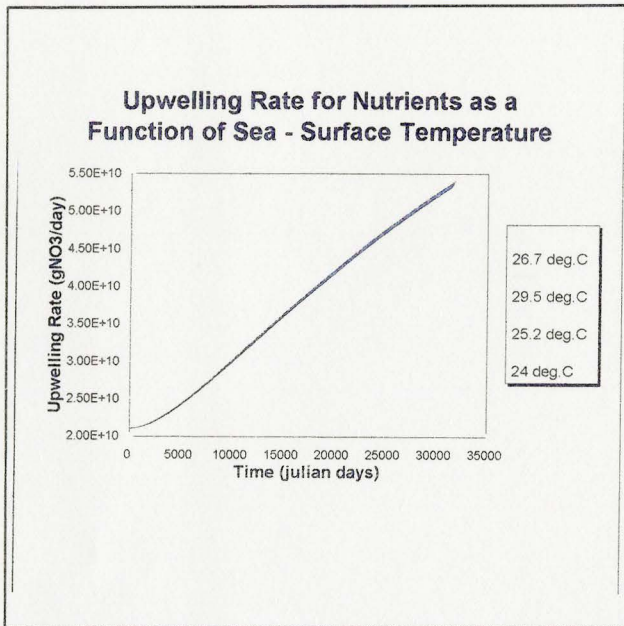


FIGURE 13a

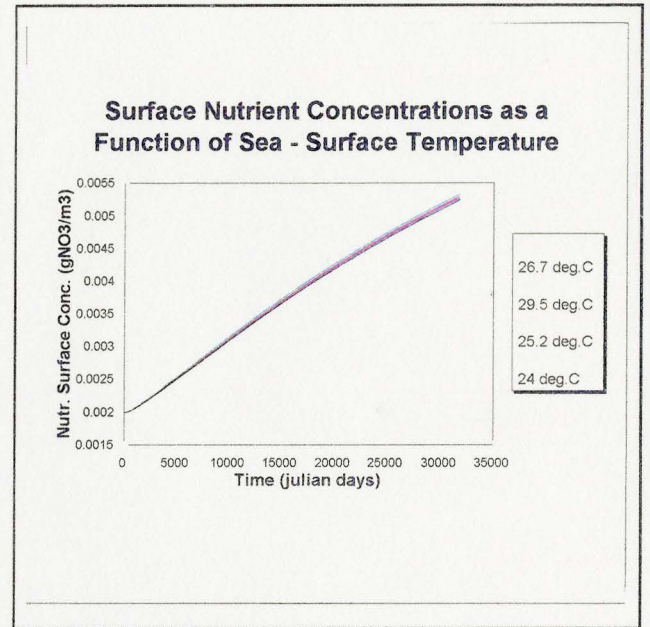


FIGURE 13b

concentrations gradually increase, linearly, over time at a rate of approximately $1 \times 10^{-7} \text{ g/m}^3 \cdot \text{day}$ or $4 \times 10^{-5} \text{ g/m}^3 \cdot \text{year}$. The pattern demonstrated here do not quite agree with measurements in the natural system. The weakening of upwelling during ENSO periods causes the nutrient concentration in the surface layer to decline significantly from that of the non-ENSO conditions (*Barber and Chavez, 1983; Feely et al., 1987, 1994, Murray et al., 1994*). However, the results of the EPCM suggest that during El Niño events (ie. maximum temperature) as well as normal conditions, surface nutrient concentration changes are minimal (ie. less than 2% change from the average).

- Organic Carbon

The sole contributor to the organic carbon content in the EPCM is zooplankton excretion. As previously mentioned, fecal matter is the primary source of particulate organic carbon (POC) in oceanic waters. The rate of zooplankton excretion is dependent upon the grazing rates of zooplankton. The

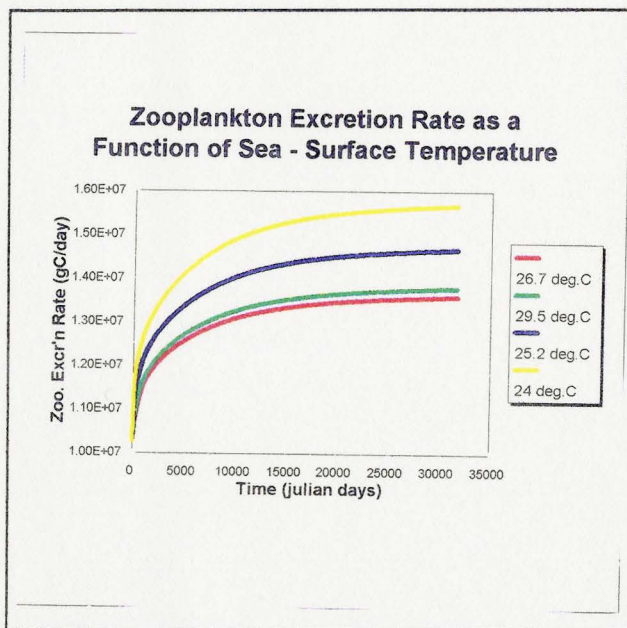


FIGURE 14a

a portion of the ingested phytoplankton that is excreted (Valiela, 1984) Figure 14a demonstrates that changes in temperature influences the zooplankton excretion rate of organic carbon. According to the EPCM, the zooplankton do not respond positively to a decrease in temperature, as shown by the maximum excretion rate at 24°C. The average SST coincides with the lowest excretion rate meaning that compared to the maximum and minimum values a greater proportion of the ingested prey is metabolized and used for growth and energy

mass that is consumed by zooplankton follows various pathways. A proportion of the filtered phytoplankton that contributes to the actual growth rate of the zooplankton is metabolized. In addition, some of that assimilated food is used toward respiration, reproduction and production. However, there is

Hence, the zooplankton are more efficient at this optimal temperature of 26.7°C. Colder and warmer temperatures work to reduce this efficiency, but the lower temperatures have a much less extreme effect on the zooplankton excretion rates. The difference between the maximum and average temperatures gave an increase in zooplankton excretion rate of approximately 15% in 1986, whereas that of the minimum SST is about 15%. Again, the response to an increase in temperature is much less (ten times) than that to a decrease in temperature. In fact, the effect of the maximum temperature is negligible.

From the above results it would be expected that simulation would give greater concentrations of organic carbon at a cooler temperature than at a warmer temperature in both the deep and the surface layers. That is exactly

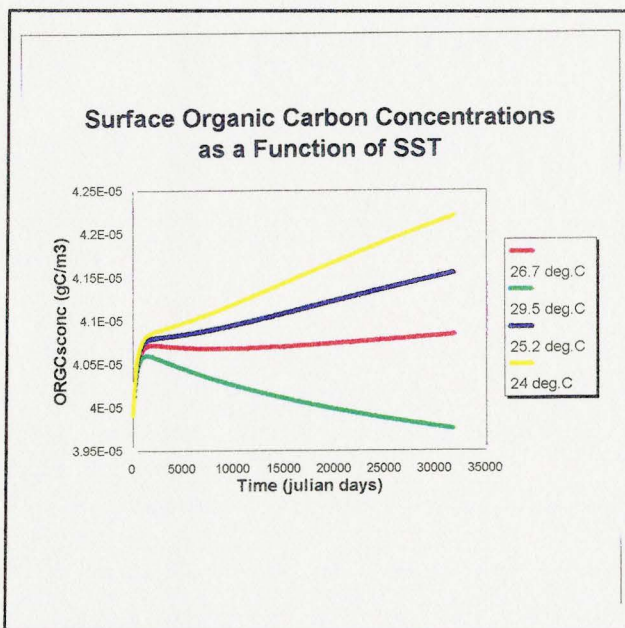


FIGURE 14b

what is observed when the output is plotted (Figure 14b) At the end of the run time, the minimum temperature coincides with a concentration of about $4.22 \times 10^{-5} \text{ g/m}^3$ whereas the concentration as a function of the maximum temperature is $3.98 \times 10^{-5} \text{ g/m}^3$ The organic carbon concentration corresponding to the average SST generally remains constant over

time. The cooler temperature of 24°C causes the concentration to progressively

increase while with the maximum temperature a decreasing trend is noticed. Hence, the high El Niño-like sea-surface temperatures may limit the organic carbon concentration in the equatorial Pacific waters. However, the maximum and minimum differences less than 3% of the reference state are quite small.

The upwelling rate for organic carbon is not affected much by high temperatures, but is more sensitive to colder temperatures. This is similar to the previous results of SST and upwelling. However, for each of the temperatures (minimum and maximum) the response is slight. The upwelling of the minimum temperature increases only by 3% from the medium value and that of the maximum temperature rises by only about 0.3%. Unlike the zooplankton concentrations, the organic carbon concentrations are not sensitive to small changes in upwelling.

- CO₂

In the EPCM, the response to changing temperatures of the CO₂ parameters is negligible (*Figures 15a to 15c*). Although individual effects of carbon dynamics, represented in the EPCM, to temperature changes may be fairly significant, the overall effect on the principal component of interest, CO₂, is slight. Lefevre et al. (1994), however, showed from measured data of the equatorial Pacific, that CO₂ does respond to SST. A negative regression was determined between the SST and surface CO₂ partial pressure (pCO₂) data. In addition, they showed a positive correlation between surface nitrate levels and

pCO₂. Both of these relationships demonstrate that El Niño conditions tend to lower sea-surface CO₂ concentrations.

The discrepancy encountered here is most likely due to an error that was eventually recognized in the model code. For these sensitivity runs, the CO₂ concentrations that were utilized were values representative of the *total* inorganic species, not just the H₂CO₃ alone. The error was corrected for in the proceeding simulations considering levels of sensitivity to changes in upwelling rate. The original terms utilized in the sensitivity runs may be found in Appendix A, Table 1. However, the majority of this study considers the “new and improved” equations that are outlined in the section on **flux between the surface and the local atmosphere**. The changes that were made to the model with respect to CO₂ fluxes could account for the 100-fold difference between the EPCM values and the expected values.

Another possible cause of the insufficient CO₂ flux and concentrations may be in relation to the coefficients utilized for death via endogenous respiration. K2 and K3, the coefficients for endogenous respiration of phytoplankton and zooplankton respectively, were adjusted in order to simulate realistic variable values. However, K2 and K3 may have been decreased too much so that negligible CO₂ could be produced for discrimination in the aqueous (and atmospheric) compartments.

Furthermore, since the local atmosphere is linked to the rest of the Earth's atmosphere in the EPCM, the changes of the equatorial Pacific are so small in

comparison to the rest of the Earth's atmosphere that the deviations in upwelling go unnoticed.

Aside from the problems of CO₂ magnitudes, the plots do demonstrate that over time oceanic CO₂ flux and concentrations increase and consequently, the atmospheric levels of CO₂ rise as well. Although the magnitudes of the CO₂ flux and concentration are deviant, the trends will most likely remain the same or similar. This increase in flux corresponds to a rate of approximately 3.82×10^{-6} g/m³·day or 2×10^{12} g/day, respectively (Figure 15c).

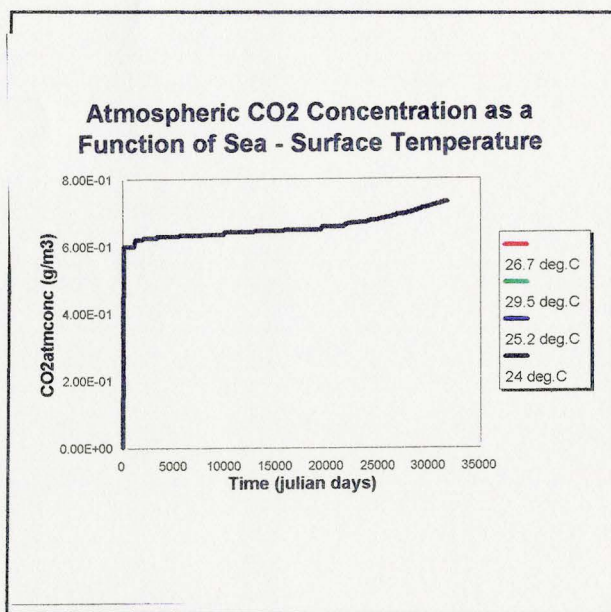


FIGURE 15a

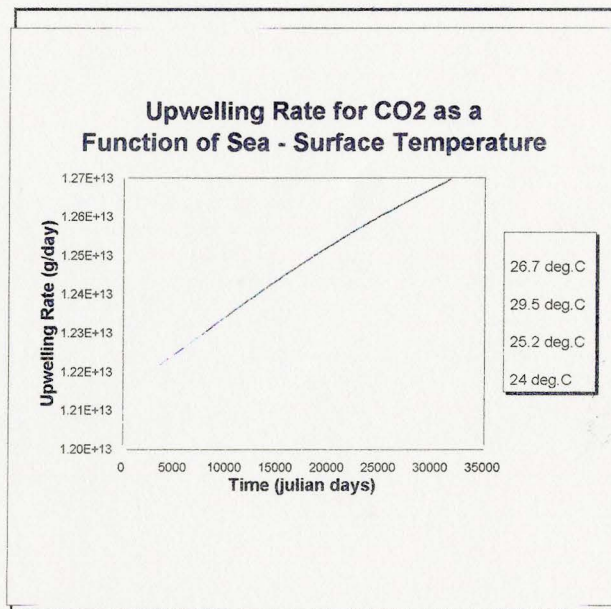


FIGURE 15b

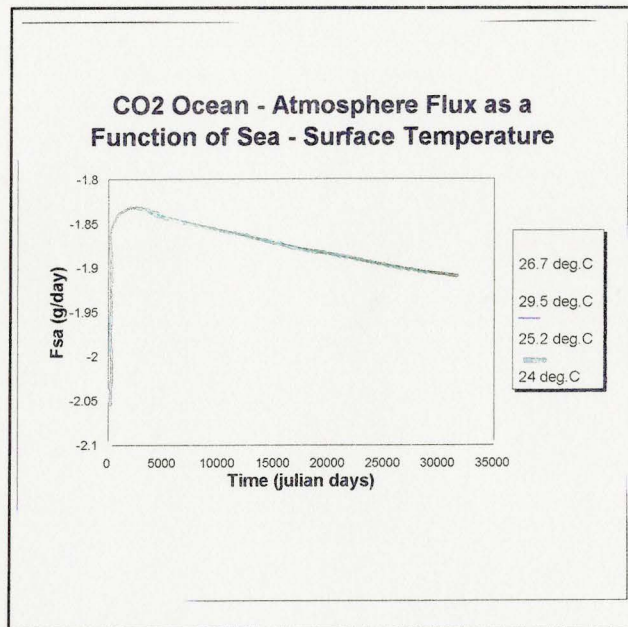


FIGURE 15c

Upwelling Effects

The second set of sensitivity tests that were performed had the purpose of determining the effects of upwelling rate on the component processes and concentrations. As mentioned previously, upwelling is an important parameter to observe in this study since it is directly related to ENSO occurrences and subsequent deviations in the distribution of carbon. El Niño has the effect of reducing the intensity of upwelling. However, the upwelling rate within the equatorial Pacific during normal conditions is not well known and, as well, the degree of reduction during ENSO periods has not yet been precisely determined (Murray *et al.*, 1994). Therefore, it was reasonable to develop a range of upwelling intensities in order to see the effect that El Niño type upwelling may

have on the environment with respect to carbon cycling. In the following runs, five different upwelling velocities, less intense than the normal condition value (0.7 m/day as used by Feely *et al.*, 1992 from Murray *et al.*, 1994) are analysed: 0.46 m/day which is two times the downwelling velocity of 0.23 m/day, 0.34 m/day at 1.5 times larger than the downwelling rate, 0.23 m/day equaling the downwelling rate, 0.12 m/day which is half the downwelling rate and finally, 1.15 m/day. The last value is five times as large as the downwelling velocity and is used simply to compare what the effect of a maximum upwelling rate would be to the other rates. The remaining conditions stayed the same as with the sea-surface temperature runs, except that temperature is kept at a maximum value of 29.5°C, again representative of El Niño conditions. As well, the upwelling velocity of 0.46 m/day was used as the standard value in these runs.

Decreased upwelling rate shows a definite decrease in both the growth

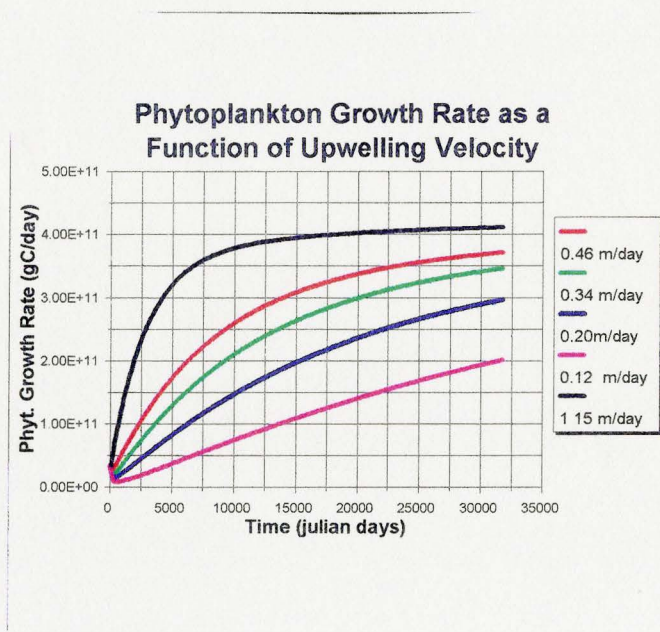


FIGURE 16A

and death rates of phytoplankton, as well as the zooplankton death rate (Figure. 16a). To exemplify the sensitivity of these rates to upwelling, when the standard upwelling velocity is decreased to 0.34 m/day, the percentage change for the growth rate is about 6%. When the upwelling rate is twice as

great as the value that is twice that of the downwelling the percentage change becomes 21% and when the upwelling rate is 0.12 m/day (or three times less than the reference value) the difference increases to 43%. So, with an increasingly weak upwelling rate the growth and death of phytoplankton and the growth of zooplankton are regulated to progressively smaller values, each time having greater intervals from the standard upwelling velocity

The zooplankton death and excretion rates (*Figure 16b*) also exhibit a similar pattern as what was just demonstrated. However, the magnitude of change, with decreasing upwelling velocity, is significantly less than the previous rates. The weakening of upwelling does not become profound until the upwelling rate is at least 0.23 m/day

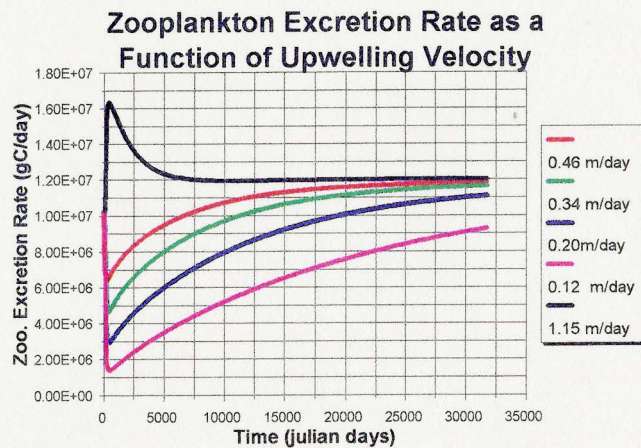


FIGURE 16b

For each of the five components, the surface and deep layer concentrations showed opposite responses to one another when changes in upwelling rate were made. In the surface layer the concentrations increased with increasing upwelling velocity (Figure 16c) However, concentrations at depths greater than 100 m decrease as upwelling rates become greater This is logical since a certain amount of the component within the deep layer is transported up to the surface, adding to the surface concentration, but eliminating a portion of the stock from the deep.

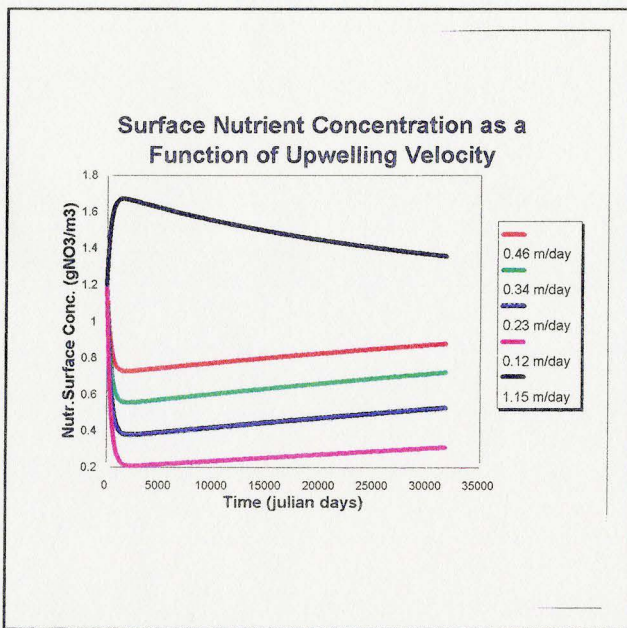


FIGURE 16c

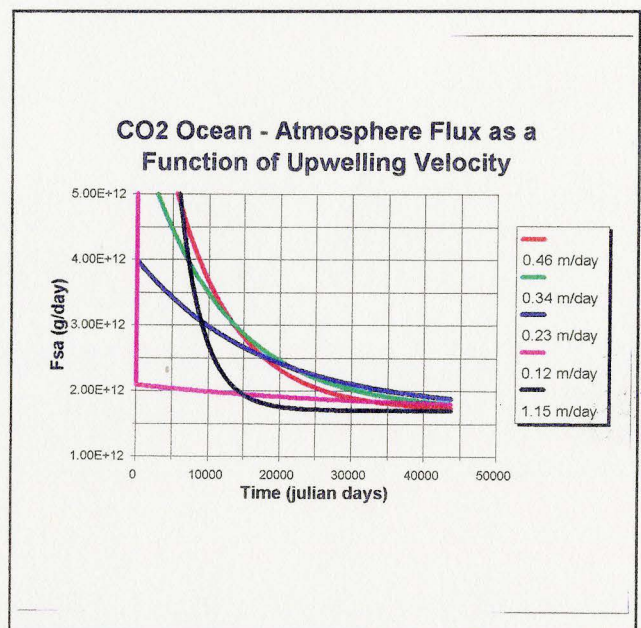


FIGURE 16d

Zooplankton concentrations are the least sensitive to changes in upwelling rate. Phytoplankton respond to a greater extent than zooplankton, but a significant effect is not observed until the upwelling rate is about two times smaller than the reference upwelling rate. Nutrient, CO₂, and organic carbon

concentrations are all equally and the most sensitive to changes in upwelling rate. A 1% decrease in upwelling rate corresponds to approximately a 20% decrease in concentration of each in the surface layer. When the upwelling rate is twice and three times as small as the standard velocity, the concentrations lessen by about 40% and 60%, respectively, from the standard upwelling rate. Thus, a significant decline (in the surface) or incline (in the deep layer) results from a lowering of intensity of upwelling rate.

Another aspect considered during these tests was the ocean-atmosphere flux of CO₂ as a function of upwelling. *Figure 16d* suggests that, according to the EPCM, the equatorial Pacific always acts as a net source of CO₂. This situation still persists even when the conditions are of the least intense upwelling rate (ie. the most abnormal conditions corresponding to an El Niño event). Therefore, the EPCM suggests that El Niño conditions are not aversive enough to reverse the direction of movement. As well, this graph (*Figure 16d*) shows that as upwelling rate increases, so does the flux to the atmosphere.

The rates of CO₂ exchange to the atmosphere is in good agreement with various observations made in the past. According to the EPCM, fluxes have an approximate order of magnitude of a gigaton which is very similar to what has been previously suggested (*Lefevre and Dandonneau, 1992; Lefevre et al., 1994; Murray et al., 1994*).

Lastly, it is noticed from *figure 16e* that unlike the previous parameter responses to upwelling, the atmospheric CO₂ levels seem to be insensitive to

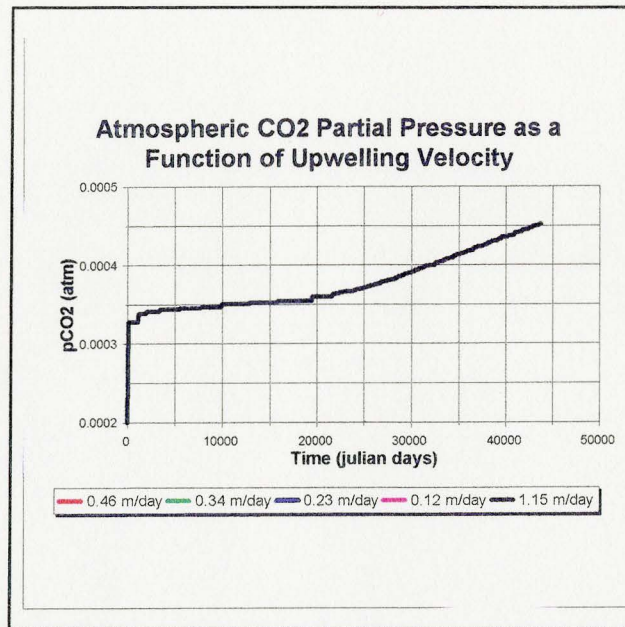


FIGURE 16e

these types of changes. This was also observed when the atmospheric CO₂ levels were taken as a function of SST. It is possible that the reason for the insensitivity of CO₂ toward upwelling changes is due to the interaction of the local atmosphere with the external atmosphere. It may be the way in which the EPCM is constructed that allows the external atmosphere to constantly compensate for changes in the amounts of CO₂ within the local atmosphere. Thus, the external atmospheric compartment may react to variations in the local atmosphere by keeping the CO₂ levels of local atmosphere at concentrations similar or the equal to levels of the rest of the Earth's atmosphere.

Historic Runs

The EPCM makes it possible to observe how certain parameters have changed over time. With the incorporation of observed field data into the model, estimates on the magnitude of variation may be determined. In this study, the parameter of interest is the atmospheric CO₂ levels and the concurring ocean-atmosphere fluxes. This will aid in the understanding of the role of the equatorial

Pacific Ocean with respect to carbon cycling and the associated global climate changes or greenhouse effects.

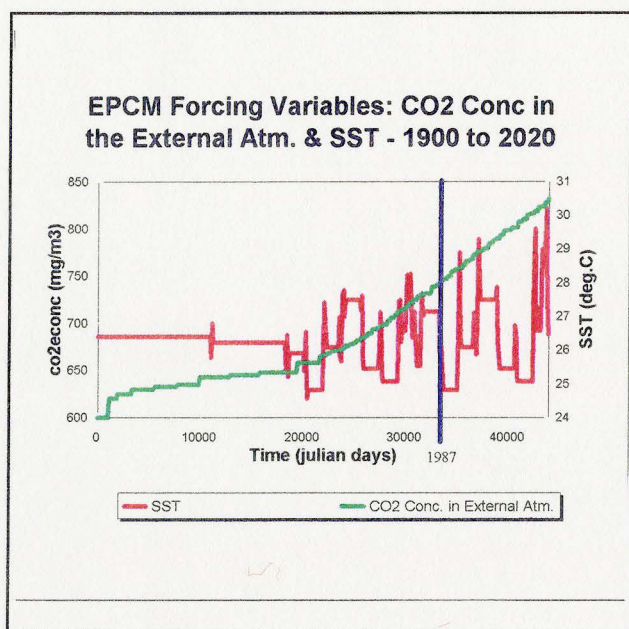


FIGURE 17a

incorporated two separate data files. The historic run incorporated two separate data files. The Earth's atmospheric CO₂ concentration and sea-surface temperature. Each of these are records of 86 years beginning at 1900. The time scale seemed appropriate since it captured the effect of the industrial revolution and deviations within the climate (ie. El Niño events). The plotting of the CO₂ concentration of the external atmosphere exhibited a gradual increasing trend in CO₂ concentration through time, where the increase is exponential in form (Figure 17a) Against this the SST record was graphed displaying an alternating peak

and trough pattern where the peaks generally represent El Niño events. When the effects of the industrial revolution begin to show in the record (ie. CO₂ concentrations begin rising at an exponential rate) the peak intensities of the SST seem to also be gradually increasing with each progressive appearance. However, if the sea-surface temperature record were to be fit with a linear line and all data points (high and low) were taken into account, a negative correlation would be observed.

No Other manipulations to the model were made. It was simply a standard simulation through time using archived records. A one hundred-day time-step was once again executed. As previously mentioned, corrections were made to the original terms relating to the CO₂ (or H₂CO₃) changes within the surface layer and the atmosphere.

The outcome of this run for local atmospheric CO₂ concentration (**CO2atmconc**) and surface-atmosphere flux (**Fsa**) demonstrated the same type of trend that was shown in the sensitivity analysis (*Figure 18ab*). As is, the EPCM shows that the atmosphere above the equatorial Pacific, since 1900, followed the trend of the external atmospheric CO₂ concentration with little, if any, differences. Thus, there is a gradual rise in CO₂ atmospheric concentration corresponding to the progressively larger flux out of the ocean surface. The change in atmospheric concentration since about 1904 and to 1986 has been about 17% which calculates to an average rate of increase of about 2×10^{12} g/day or 8×10^{14} g/year. The flux increased slowly as well from the beginning of the

century until the present time. The change was small (~3%), but still presented an increase.

The partial pressures of the local atmosphere that were simulated by the EPCM, values less than 400 μatm are in agreement with observed values (Lefevre et al., 1994 - Figure 18a) . As well, figure 18b displays a decreasing H_2CO_3 concentration with time. This occurs because the way in which the EPCM is constructed. As the H_2CO_3 concentration within the surface layer surpasses the equilibrium H_2CO_3 concentration, the movement of inorganic carbon is in the direction of the atmosphere (refer to Figure 18a). Since the ocean-atmosphere flux is taking away from the surface stock of H_2CO_3 throughout time, the amount of surface inorganic carbon in the ocean is slowly decreasing. This may also be the reason why the ocean-atmosphere flux of CO_2 gradually decreases over time (ie. There is increasingly less inorganic carbon at the sea surface).

Figure 18a also demonstrates that over the 86 year period, the equatorial Pacific has always been a source of CO_2 , but has decreased as time continued. Flux rates began at 1.2×10^{13} g/day and in 1986 were approximately 1.5×10^{12} g/day. According to the EPCM, the period of time around 1986 indicates that flux to the atmosphere leveled off and reached a sort of steady-state condition.

Business As Usual - A Look into the Foreseeable Future

Modelling is not only useful for the purpose of observing past trends in environmental system variations, but also for predicting futuristic outcomes.

What will the atmospheric CO₂ levels be like in the future? Will the ocean-atmosphere fluxes ever vary? Will they change to such an extreme that the oceans will actually uptake CO₂ instead of releasing it? These are the types of questions that can potentially be answered with the use of a model and which will be investigated here. It is desirable to hypothesize what the fairly immediate effect the equatorial Pacific will have on the atmospheric CO₂ levels, since "today's environment" is what seems to be of primary concern to most of mankind.

The data files that were used for the historic runs contained records from the beginning of this century until 1986. With respect to the external atmospheric CO₂ concentration data, by 1960 the apparent trend is a continuous increase in CO₂ levels with time. Hence, these values were extrapolated in order to have a reasonable CO₂ data file that includes futuristic data points.

The SST data was not as consistent. The record fluctuated much more during that allocated time span and it was more difficult to identify a consistent trend. Because of that, the data points from day 20 000 and on were repeated (ie. the values beginning at 1900 were recycled) with exception of the major peaks. As mentioned previously, it can be noticed in *Figure 17a* that the primary peaks of the SST graph are progressively getting larger and seemingly, the differences between each peak and it's predecessor is approximately 0.3°C. Thus, the values to extrapolated from the SST data record were based on these characteristics.

Figure 17a shows the extrapolated data points from 1987 and on for both the SST and the external CO₂ concentration files. It is assumed that the trends observed in the present and the past will continue along the same or similar path. Figure 18b simply shows that the pCO₂ levels of the atmosphere continue to

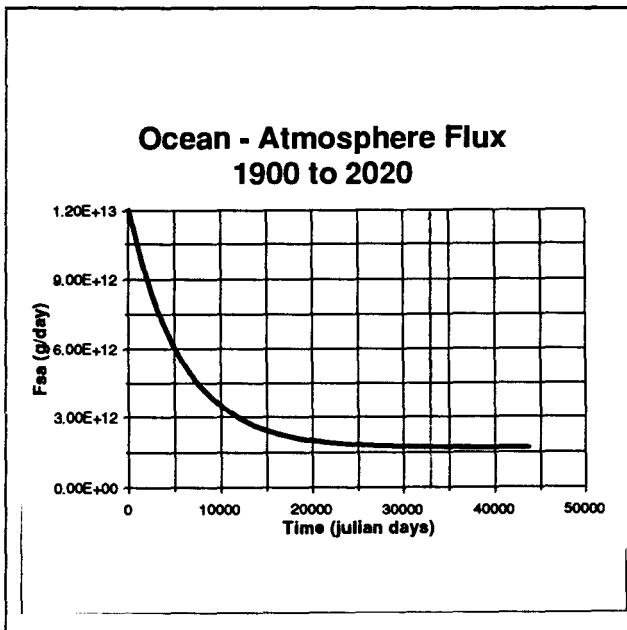


FIGURE 18a

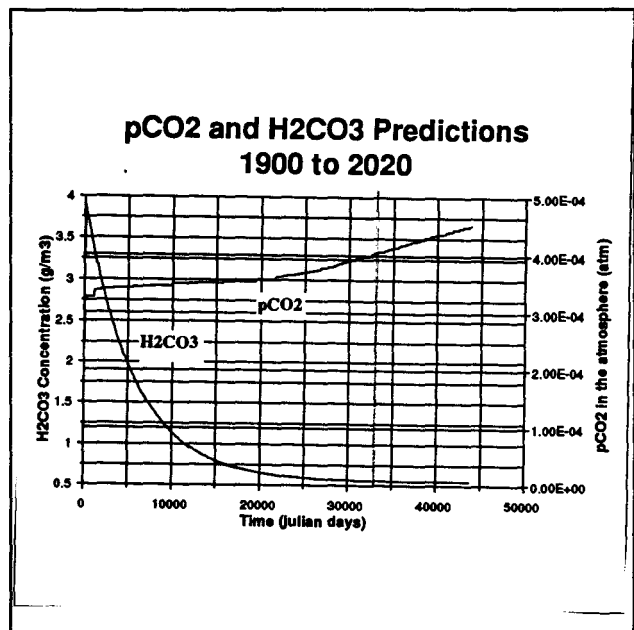


FIGURE 18b

increase and reaches a level close to 450 μ atm by year 2020. Thus, EPCM predicts that the change, in atmospheric CO₂ levels above the equatorial Pacific, from 1986 to the year 2020 is approximately 12.5% which corresponds to a rate of increase of 1.47 μ atm /day.

In contrast, the ocean-atmosphere flux out of the surface water to the atmosphere is predicted to continue to decrease until the year 2020 where rates

will be about 1.5 g/day. After 1986 there is still no indication, according to the EPCM, of a reversal in flux direction (*Figure 18a*).

(6) Discussion and Conclusions

An obvious and consistent trend of each of the simulation runs is that the components were at least 10% less sensitive to maximum temperatures as compared with minimum sea-surface temperatures. In all cases, warmer sea-surface temperatures, similar to those of El Niño periods, have percentage changes from the average which are very small and possibly even arbitrary. With respect to temperature ranges, the equatorial Pacific carbon cycle may vary more from the average with temperature minimums than with temperature maximums. Therefore, periods of anomalously cool temperatures, like La Niña events which alternate with the warm El Niño periods, may result in greater deviations from the norm compared to the warm ENSO periods. Traditionally, El Niño events have been the focus of climatic deviations having a large effect on oceanic systems of the equatorial region (*Feely et al., 1987, 1994; Murray et al., 1994*). However, according to the EPCM, anomalously cool temperatures may be more of a concern, on a short-term basis, with respect to CO₂ releases into the atmosphere. Upwelling tends to be more intense during cooler periods and subsequently, surface water CO₂ concentrations are larger and the rate of diffusion of CO₂ into the local atmosphere increases.

In the past it has been felt that biological parameters, because of their large contribution to the carbon cycle, were strongly influenced by climatic deviations causing anomalous CO₂ levels in the equatorial Pacific Ocean and the atmosphere. However, the EPCM has suggested that the components are weakly sensitive to temperature changes most often accompanying short-term climatic changes such as the El Niño. The majority of the components and their processes demonstrated no greater than 5% changes from the norm with the exception of zooplankton concentrations which exhibited an approximate change of 15%.

The components are sensitive to changes in upwelling, a physical oceanic process. Weak upwelling velocities, about 1.5 or less times that of downwelling, in all cases produced percentage changes ranging from approximately 20% to 40%. Therefore, the EPCM is in agreement with the statement of Murray et al. (1994) concluding that physical processes control the CO₂ flux of the eastern equatorial Pacific. So, in order to get more accurate estimates of rates and stocks the EPCM may need to incorporate a more specific and intense changing of upwelling rate over time (ie. Rates corresponding more typically with El Niño events) since the temperature changes did not create changes in upwelling to cause great effects on the components. This may entail the addition of more mechanisms which affect upwelling, such as the influence of surface winds, especially during anomalous conditions.

The EPCM reproduces many of the results of earlier studies. Previously, it has been recorded that the warmer temperatures characteristic of El Niño events

coincide with weakening of upwelling intensity (*Freely et al., 1987, 1994*). The same effect is seen with the EPCM, but the model changes in upwelling with temperature are small. However, the carbon stocks seem to be sensitive to upwelling rates. This is observed in both of the sensitivity runs. If the weakening of upwelling velocity results in rates closer to the downwelling rates (ie. at least 1.5 times the downwelling velocity), concentration changes may be large enough to create significant oceanic concentration changes.

The ocean-atmosphere flux of CO₂ into the atmosphere is positively correlated with upwelling. The upwelling mechanism transports CO₂ from the deep layer up to the surface hence, conditions where the upwelling rate is greatest (ie. normal non-El Niño conditions) will correspond to high CO₂ concentrations in the surface layer. Consequently, movement in the direction of the atmosphere will predominate. As well, the EPCM has estimated a flux of CO₂ ranging from approximately 0.6 to 0.5 gigatons of carbon per year in the 1980's which is within the range of the observed rates (0.6 to 0.9 gigatons per year - *Lefevre et al., 1994; Lefevre and Dandonneau, 1992; Murray et al., 1994*). Furthermore, the flux always occurs in the direction towards the local atmosphere. Even when the conditions were set to be maximally deviated and simulated for the entire 86 years in this manner, a reversal of direction never occurred. Hence, if the El Niño conditions of the natural system are within the range of what has been modelled, the equatorial Pacific will always be a source of CO₂ to the atmosphere. ENSO does not produce conditions extreme enough

to severely upset the system. If, however, CO₂ continues to accumulate in the atmosphere and these levels become extremely high, movement in the direction of the ocean may occur, in which case the equatorial Pacific may act as a sink for CO₂. However, the trend that is suggested by the EPCM is that the equatorial Pacific is and will remain a net source of CO₂ to the atmosphere. The actions of El Niño, as defined by the EPCM, do not seem to be strong enough to reverse the direction of flux.

In conclusion, the EPCM demonstrated three significant trends. First, the sensitivity analysis testing the effects of both sea-surface temperature and upwelling rate changes on the model parameters suggested that upwelling has a large effect whereas the effect of sea-surface temperatures on the dynamic cycling of carbon is negligible.

Secondly, the EPCM verified that it is the physical processes that are responsible for the majority of parameter changes within the eastern equatorial Pacific region. Since the exact changes in upwelling intensity during ENSO periods are essentially unknown, it is impossible to determine the exact effect of the El Niño events. However, the EPCM did demonstrate that the carbon cycle of the equatorial Pacific is more sensitive to cooler temperatures than warmer temperatures (as compared to the average SST). Thus, it may very well be that the El Niño has only a small effect on the outflux of CO₂ into the atmosphere and may not be enough to severely perturb the system. Subsequently causing a reversal in CO₂ movement between the ocean and the atmosphere.

Futuristic runs predict that atmospheric CO₂ concentrations above the equatorial Pacific are increasing at a rate of 1.47 μatm/day and may reach 450μatm by the year 2020. In addition, the EPCM suggested that the equatorial Pacific is always a continual source of CO₂ to the atmosphere where the flux has a magnitude of approximately 0.5 to 0.6 gigatons per year.

REFERENCES

- Barber, R.T. and Chavez, F.P. (1986) Ocean variability in relation to living resources during the 1982-83 El Niño. *Nature*, 319:279-285.
- Barber, R.T. and Chavez, F.P. (1983) Biological consequences of El Niño. *Science*, 222:1203-1210.
- Bishop et al. The chemistry, biology, and vertical flux of particulate matter of the Panama Basin.
- Bolin, B. (1981) *Carbon Cycle Modelling - Scope 16*. Toronto:John Wiley & Sons.
- Butchers, S.S. et al., (1992) *Global Biogeochemical Cycles*. Toronto:Academic Press - Harcourt Brace, Jovanovich Publishers.
- Cole, J.E. and Fairbanks, R.G. (1990) The southern oscillation recorded in the 1800s of corals from Tarawa Atoll. *Paleoceanography*, 5(5):669-683.
- De Baar, H.J.W. and Suess, E. (1993) Ocean carbon cycle and climate change - an introduction to the interdisciplinary union symposium. *Global and Planetary Change*, 8:vii-x.
- Diaz, H.F. and Kiladis, G.N. (1992) The atmospheric teleconnections associated with the extreme phase of the Southern Oscillation. In *El Nino - Historical and Paleoclimatic Aspects of the Southern Oscillation*. (Eds. Diaz, H.F. and Markgraf, V.) New York, NY:Cambridge University Press. Pp.7-28.
- Di Toro et al. (1971) A Dynamic Model of the Phytoplankton Population in the Sacramento-San Joaquin Delta in *Nonequilibrium Systems in Natural Water Chemistry - Advances in Chemistry Series 106*. Washington, D.C.:American Chemical Society. pp.121-180.
- Fasham, M.J.R. et al., (1990) A nitrogen-based model of plankton dynamics in the oceanic mixed layer. *Journal of Marine Research*, 48:591-639.
- Feely, R.A. et al. (1987) Distribution of chemical tracers in the eastern equatorial Pacific during and after the 1982-1983 El Niño/Southern Oscillation event. *Journal of Geophysical Research*, 92(C6):6545-6558.

- Feely, R.A. et al. (1994) The effect of tropical instability waves on CO₂ species distributions along the equator in the eastern equatorial Pacific during the 1992 ENSO event. *Geophysical Research Letters*, 21(4):277-280.
- Fielder, P.C. et al. (1991) Oceanic upwelling and productivity in the eastern tropical Pacific. *Limnology and Oceanography*, 36(8):1834-1850.
- Gouriou, Y. And Toole, J. (1993) Mean circulation of the upper layers of the western equatorial Pacific Ocean. *Journal of Geophysical Research*, 98(C12):22,495-22,520.
- Klepper, O. et al. (1994) *Biochemical feedbacks in the oceanic carbon cycle. Ecological Modelling*, 75/76:459-469.
- Knauss, (1978) Introduction to Physical Oceanography. Englewoodcliffs, N.J.:Prentice-Hall, Inc.
- Lefevre, N. et al. (1994) PCO₂, chemical properties, and estimated new production in the equatorial Pacific in January-March 1991. *Journal of Geophysical Research*, 99:12639-12654.
- Lefevre, N. And Dandonneau, Y. (1992) Air-sea CO₂ fluxes in the equatorial Pacific in January-March 1991. *Geophysical Research Letters*, 19(22):2223-2226.
- Longhurst, A.R. (1991) Role of the marine biosphere in the global carbon cycle. *Limnology and Oceanography*, 36(8):1507-1526.
- McCreary, J.P. and Lu, P. (1994) Interaction between the subtropical and equatorial ocean circulations: the subtropical cell. *Journal of Physical Oceanography*, 24:466-496.
- Murray, J.W. et al. (1994) Physical and biological controls on carbon cycling in the equatorial Pacific. *Science*, 266:58-65.
- Murray, J.W. et al. (1989) Nutrient assimilation, export production and ²³⁴Th scavenging in the eastern equatorial Pacific. *Deep-Sea Research*, 36(10):1471-1489.
- Parsons, T.R. et al. (1984) *Biological Oceanographic Processes*. 3rd Edition. Willowdale, Ontario:Pergamon Press Canada Ltd.
- Peterson, E.E. (1965) *Chemical Reaction Analysis*. Englewood Cliffs, N.J.:Prentice-Hall.
- From IAWPRC Task Group on Mathematical Modelling for Design and Operation of Biological Wastewater Treatment. (1987) Activated Sludge Model No.1. Scientific and Technical Report No. 1. Great Britain, Bristol:J.W. Arrowsmith Ltd

- Philander, S.G.H. et al. (1987) Simulation of the seasonal cycle of the tropical Pacific Ocean. *Journal of Physical Oceanography*, 17:1986-2002.
- Picaut, J. And Tournier, R. (1991) Monitoring the 1979-1985 equatorial Pacific current transports with expendable bathythermograph data. *Journal of Geophysical Research*, 96:3263-3277.
- Ramage, C.S. (1986) El Nino. *Scientific American*, 254:76-83.
- Sarmiento, J.L. (1993) Ocean Carbon Cycle. *C&EN*. May 31.
- Siegenthaler, U. and Sarmiento, J.L. (1993) Atmospheric carbon dioxide and the ocean. *Nature*, 365:119-125.
- Smith, S.V. and Hollibaugh, J.T. ((1993) *Coastal metabolism and the oceanic organic carbon balance*.
- Stumm, W. And Morgan, J.J. (1970) *Aquatic Chemistry; an introduction emphasizing chemical equilibria in natural waters*. New York: Wiley-Interscience
- Thurman, H.V. (1989) *Introductory Oceanography*. 6th Edition. Toronto:Collier Macmillan Canada, Inc.
- Valiela, I. (1984) *Marine Ecological Processes*. New York, NY:Springer-Verlag New York, Inc.
- Wanninkhof, R. (1992) Relationship between wind speed and gas exchange over the ocean. *Journal of Geophysical Research*, 97(C5):7373-7382.

APPENDIX A

TABLE 1
EPCM: VARIABLES

SYMBOL	VARIABLE NAME	EQUATION	UNITS
GSAT	saturated growth rate of phytoplankton	$K1*TEMP*PHYTs$	gC/day
SS	self-shading term - limitation of phytoplankton growth	$Ke+(K*((PHYTs*1000)/Vs))$	m^{-1}
LT	limitation of phytoplankton growth rate by light intensity and depth	$((2.718*f)/(SS*DPTH))*(EXP(-(I_0/I_s)*EXP(-(SS*DPTH)))-EXP(-(I_0/I_s)))$	-
LIMNUT	limitation of phytoplankton growth by nutrient availability	$NUTs/(KM+NUTs)$	-
P1	phytoplankton growth rate	$GSAT*LT*LIMNUT$	gC/day
P2	phytoplankton death rate due to endogenous respiration	$K2*TEMP*PHYTs$	gC/day
P3	growth rate of zooplankton or death rate of phytoplankton due to grazing by zooplankton	$((CG*ZOOs*PHYTs)*(PHYTs/(KMP+PHYTs)))/Vs$	gC/day
P4	death rate of zooplankton due to endogenous respiration	$K3*TEMP*ZOOs$	gC/day
P5	excretion rate of zooplankton	$((CG*ZOOs*PHYTs)*(1-(PHYTs/(KMP+PHYTs))))/Vs$	gC/day
R1	reaction term for phytoplankton	$P1-P2-(P3/Y)$	gC/day

R2	reaction term for zooplankton	$P3-P4-P5$	gC/day
R3	reaction term for nutrients	$((U*P2)+(Z*P4)+(Z*P5))-(U*P1)$	gC/day
R4	reaction term for CO ₂	$(P2+P4)-P1$	gC/day
R5	reaction term for organic carbon	$P5$	gC/day
Wup1	upwelling rate for phytoplankton	$(vWup*A*PHYTdeep)/Vdeep$	gC/day
Wup2	upwelling rate for zooplankton	$(vWup*A*ZOOdeep)/Vdeep$	gC/day
Wup3	upwelling rate for nutrients	$(vWup*A*NUTdeep)/Vdeep$	gC/day
Wup4	upwelling rate for CO ₂	$(vWup*A*CO2deep)/Vdeep$	gC/day
Wup5	upwelling rate for organic carbon	$(vWup*A*ORGCdeep)/Vdeep$	gC/day
Wdown1	downwelling rate for	$(vWdown*A*PHYTs)/Vs$	gC/day
Wdown2	downwelling rate for	$(vWdown*A*ZOOs)/Vs$	gC/day
Wdown3	downwelling rate for	$(vWdown*A*NUTs)/Vs$	gC/day
Wdownw	downwelling rawe for	$(vWdown*A*CO2s)/Vs$	gC/day
Wdown5	downwelling rate for	$(vWdown*A*ORGCs)/Vs$	gC/day
EUC1	horizontal advection into the deep layer for phytoplankton	$Qin*PHYTin$	gC/day
EUC2	horizontal advection into the deep layer for zooplankton	$Qin*ZOOin$	gC/day
EUC3	horizontal advection into the deep layer for nutrients	$Qin*NUTin$	gC/day
EUC4	horizontal advection into the deep layer for CO ₂	$Qin*CO2in$	gC/day

EUC5	horizontal advection into the deep layer for organic carbon	$Q_{in} * ORGC_{in}$	gC/day
OUT1	horizontal advection out of the surface layer for phytoplankton	$(Q_{out} * (PHYTs/Vs))$	gC/day
OUT2	horizontal advection out of the surface layer for zooplankton	$(Q_{out} * (ZOOs/Vs))$	gC/day
OUT3	horizontal advection out of the surface layer for nutrients	$(Q_{out} * (NUTs/Vs))$	gC/day
OUT4	horizontal advection out of the surface layer for CO ₂	$(Q_{out} * (CO2s/Vs))$	gC/day
OUT5	horizontal advection out of the surface layer for organic carbon	$(Q_{out} * (ORGCs/Vs))$	gC/day
PCO2	partial pressure of CO ₂ of the surface water	$(CO2_{atm}/V_{atm}) * (1/pureCO2)$	atm
H2CO3eq	equilibrium concentration of H ₂ CO ₃	$KH * pCO2 * density$	mol/kg
H	pH for the system	$H2CO3eq / K'1 * ALK$	-
H2CO3t	non-equilibrium H ₂ CO ₃ concentration	$CO2s * K'1 / (H + K'1) *$ (conversion from mol/m ³ to mol/kg)	mol/kg
HC	difference between equilibrium H ₂ CO ₃ concentration and non-equilibrium H ₂ CO ₃ concentration	$H2CO3t - H2CO3eq$	

Fsa	flux of CO ₂ between the surface and the local atmospheric layers	$HC \cdot (D/A)$	gC/day
Fae	flux of CO ₂ between the local atmosphere and the rest of the Earth's atmosphere	$((HD \cdot ((CO_2_{conc}/1000) - (CO_2_{atm}/V_{atm}))) / A_x) \cdot V_{atm}$	gC/day
PHYTs	stock of phytoplankton in the surface layer	$W_{up1} - (W_{down1} + OUT_1) + R_1$	gC
ZOOs	stock of zooplankton in the surface layer	$W_{up2} - (W_{down2} + OUT_2) + R_2$	gC
NUTs	stock of nutrients in the surface layer	$W_{up3} - (W_{down3} + OUT_3) + R_3$	gC
CO2s	stock of CO ₂ in the surface layer	$W_{up4} - (W_{down4} + OUT_4) + R_4$	gC
ORGCs	stock of organic carbon in the surface layer	$W_{up5} - (W_{down5} + OUT_5) + R_5$	gC
PHYTdeep	stock of phytoplankton in the deep layer	$EUC_1 + W_{down1} - W_{up1} + R_1$	gC
ZOOdeep	stock of zooplankton in the deep layer	$EUC_2 + W_{down2} - W_{up2} + R_2$	gC
NUTdeep	stock of nutrients in the deep layer	$EUC_3 + W_{down3} - W_{up3} + R_3$	gC
ORGCdeep	stock of organic carbon in the deep layer	$EUC_5 + W_{down5} - W_{up5} + R_5$	gC
CO2deep	stock of CO ₂ in the deep layer	$EUC_4 + W_{down4} - W_{up4} + R_4$	gC
CO2atm	stock of CO ₂ in the local atmosphere	$Fae - Fsa + R_4$	gC
PHYTsconc	concentration of phytoplankton in the surface layer	$PHYTs/V_s$	gC/m ³

ZOOsconc	concentration of zooplankton in the surface layer	ZOOs/Vs	gC/m ³
NUTsconc	concentration of nutrients in the surface layer	NUTs/Vs	gC/m ³
CO2sconc	concentration of CO ₂ in the surface layer	CO2s/Vs	gC/m ³
ORGCsconc	concentration of organic carbon in the surface layer	ORGCs/Vs	gC/m ³
PHYTdconc	concentration of in the deep layer	PHYTdeep/Vdeep	gC/m ³
ZOOdconc	concentration of in the deep layer	ZOOdeep/Vdeep	gC/m ³
NUTdconc	concentration of in the deep layer	NUTdeep/Vdeep	gC/m ³
CO2dconc	concentration of in the deep layer	CO2deep/Vdeep	gC/m ³
ORGCdconc	concentration of in the deep layer	ORGCdeep/Vdeep	gC/m ³
CO2atmconc	concentration of in the deep layer	CO2atm/Vatm	gC/m ³

APPENDIX B

TABLE 2
EPCM: CONSTANTS

SYMBOL	CONSTANT NAME	VALUE	UNITS
K1	doubling of saturated growth rate for a temp change from 10-20°C	0.10	(day-°C) ⁻¹
DPTH	depth of surface layer	100	m
lo	average light intensity over f (at the surface)	800	ly/day
Km	half saturation constant for phytoplankton growth	2.629 x 10 ¹¹	gNO ₃
K2	endogenous respiration constant for phytoplankton	0.00185	(day-°C) ⁻¹
f	photoperiod	0.5	-
Is	optimum light intensity for phytoplankton growth	113.4	ly/day
Y	utilization efficiency	0.63	gCPHYT/gCZOO
K3	zoopl. endogenous respiration constant	0.0004	(day-°C) ⁻¹
Z	nutrient to zooplankton biomass concentration ratio	0.19	gNO ₃ /gC
U	nutrient to phytoplankton biomass concentration ratio	0.17	gNO ₃ /gC
KMP	Michaelis constant for zooplankton growth	1 X 10 ¹¹	gC/m ³
CG	filtering rate of zooplankton	0.84	m ³ /gC-day ⁻¹

SYMBOL	CONSTANT NAME	VALUE	UNITS
Ke	extinction coefficient due to particulates, suspended matter, etc.	0.78	m ⁻¹
K	extinction coefficient due to phytoplankton biomass	0.02	m ⁻¹
TEMP	temperature (SST)	26.4	°C
vWup	upwelling velocity	0.7	m/day
A	area of study region	4.31 x 10 ¹³	m ²
Vs	volume of surface layer	4.31 x 10 ¹⁵	m ³
vWdown	downwelling velocity	0.23	m/day
Vdeep	volume of deep layer	1.72 x 10 ¹⁷	m ³
Qin	influent flow (via EUC)	3.26 x 10 ¹²	m ³ /day
PHYT _{in} (check)	phytoplankton concentration entering the deep layer	0.002	gC/m ³
ZOO _{in}	zooplankton concentration entering the deep layer	0.004	gC/m ³
NUT _{in}	nutrient concentration entering the deep layer	0.0001	gNO ₃ /m ³
CO2 _{in}	CO2 concentration entering the deep layer	0.5	gC/m ³
ORGC _{in}	organic carbon concentration entering the deep layer	0.0001	gC/m ³
Qout	outflow (via SEC)	1.45 x 10 ¹²	m ³ /day
HC	Henry's Law constant (at 25°C, 19% Cl)	10 ^{-1.53}	mol/l·atm
K ₁	first acidity constant	10 ⁻⁶	-
ALK	alkalinity corrected for borate concentration	0.00224	mol/kg

SYMBOL	CONSTANT NAME	VALUE	UNITS
pCO ₂	partial pressure of CO ₂ in the atmosphere	407	μatm
MMh ₂ co ₃	molar mass of H ₂ CO ₃	60	gH ₂ CO ₃ /mole
co ₂ econc	concentration of CO ₂ in the rest of the Earth's atmosphere	600	mgC/m ³
HD	horizontal diffusivity coefficient	4.18176 x 10 ¹⁰	m ² /day
D	diffusion coefficient	1.425 x 10 ⁻⁴	m ² /day
MEco ₂	mass of CO ₂ in the Earth's atmosphere	2.1 x 10 ¹⁵	g
Ve	volume of the Earth's atmosphere	3.975 x 10 ¹⁸	m ³
Vatm	volume of local atmosphere	5.172 x 10 ¹⁷	m ³
Ax	cross-sectional area of the atmosphere	3.19 x 10 ¹⁰	m ²
pureCO ₂	concentration of pure (100%) CO ₂ having a pCO ₂ of 1 atm.	1833	gC/m ³
iPHYTs	initial phytoplankton stock in the surface layer	3.06 x 10 ¹²	gC
iZOOs	initial zooplankton stock in the surface layer	1.54 x 10 ¹³	gC
iNUTs	initial nutrient stock in the surface layer	6.45 x 10 ¹¹	gNO ₃
iCO ₂ s	initial CO ₂ stock in the surface layer	3.67 x 10 ¹⁵	gC
iORGs	initial organic carbon stock in the surface layer	1.253 x 10 ¹¹	gC
iPHYTdeep	initial phytoplankton stock in the deep layer	3.44 x 10 ¹³	gC

SYMBOL	CONSTANT NAME	VALUE	UNITS
iZOOdeep	initial zooplankton stock in the deep layer	1.38×10^{14}	gC
iNUTdeep	initial nutrient stock in the deep layer	6.45×10^{13}	gNO ₃
iCO2deep	initial CO ₂ stock in the deep layer	7.95×10^{16}	gC
iORGdeep	initial organic carbon stock in the deep layer	2.56×10^{12}	gC
iCO2atm	initial CO ₂ stock in the atmosphere	1.80×10^{15}	gC
iCO2earth	initial CO ₂ concentration in the Earth's atmosphere	0.0325	gC/m ³

APPENDIX C

TABLE 3
EPCM: STEADY-STATE STOCKS
NEW INITIAL VALUES

STOCK	VALUE	UNITS
PHYTs	6.90×10^{11}	gC
PHYTdeep	2.72×10^{13}	gC
ZOOs	6.03×10^{11}	gC
ZOOdeep	4.64×10^{13}	gC
NUTs	8.62×10^{12}	gNO ₃
NUTdeep	1.20×10^{14}	gNO ₃
CO2s	5.17×10^{15}	gC
CO2deep	6.88×10^{16}	gC
ORGCs	1.72×10^{11}	gC
ORGCdeep	2.58×10^{12}	gC

Appendix D

Equatorial Pacific Carbon Model Source Code Listing (GPS-X Version 2.1.1)

Listing of input parameters

!MENU ITEM: !CONSTANTS

!HEADER:!CONSTANTS

constant K1=0.1 !doubling of saturated growth rate for a 10 deg.temp change! (day-deg.C)⁻¹

constant DPTH=100 !depth of segment !m

constant Io=800 !average light intensity over f (at surface) !ly/day

constant Km=2.629E11 !Michaelis constant for phyto. growth !gNO₃

constant K2=0.00185 !endogenous respiration constant !(day-deg.C)⁻¹

constant f=0.5 !photoperiod !-

constant Is=113.4 !optimum light intensity for phyt growth !ly/day

constant K3=0.0004 !zooplankton endogenous respiration constant !(day-deg.C)⁻¹

constant KMP=1E11 !(?)Michaelis constant for zoopl. growth !gC

constant CG=0.84 !avg. filtering rate of zooplankton !m³/gC-day

#constant temp=26.4 !average SST !deg. C

constant U=0.17 !nutrient to phyt biomass conc. ratio !gNUT/gC

constant Z=0.19 !nutrient to zoo biomass conc. ratio !gNUT/gC

constant Y=0.63 !utilization efficiency !gCphyt/gCzoo

constant Ke=0.78 !extinction coefficient due to other things !m⁻¹

constant k=0.02 !extinction coefficient due to phyt !m⁻¹

constant vWup=0.7 !upwelling velocity !m/day

constant A=4.31E13 !area of study region !m²

constant Vs=4.31E15 !volume of surface layer !m³

constant vWdown=0.23 !downwelling velocity (assume for now) !m/day

constant Vdeep=1.72E17 !volume of deep layer !m³

constant Qout=1.45E12 !outflow !m³/day

constant Qin=3.26E12 !inflow !m³/day

constant PHYTin=0.02 !(?)phyt conc. entering deep layer !gC/m³

constant ZOOin=0.004 !(?)zoo conc. entering the deep layer !gC/m³

constant NUTin=0.0001 !nutrient conc. entering the deep layer !gNUT/m³

constant CO₂in=0.5 !CO₂ conc. entering the deep layer !gNUT/m³

constant ORGCin=0.00001 !organic conc. entering the deep layer !gC/m³

constant HC=0.216 !Henry's Law constant at 25 deg.C, 19% Cl-!mol/l/atm

constant MMCO₂=44 !molar mass of CO₂ !g/mole

constant D=1.425E-4 !diffusion coefficient !m²/day

constant HD=41817.6E6 !horizontal diffusivity coefficient !m²/day

constant Ax=3.19E10 !cross-sectional area of atmosphere !m²

constant pureCO₂=1833 !pure co₂ concentration (100%) !gC/m³

constant co₂econc=600 !co₂ conc in the earth's atmosphere !mg/m³

constant MEco₂=2.1E15 !mass of CO₂ in Earth !g

constant Ve=3.975E18 !volume of the Earth's atmosphere !m³

constant Vatm=5.172E17 !volume of local atmosphere !m³

Listing of output (calculated) variables

!MENU ITEM: !VARIABLES

!HEADER: !VARIABLES

display SS !self-shading effect !m-1

display GSAT !saturated growth rate of phyt !gC/day

display LT !limitation on sat. growth of phyt by light !-

display LIMNUT !limitation on sat. growth of phyt by avail. nut. !-

display P1 !phyt growth rate !gC/day

display P2 !phyt death due to end. respiration !gC/day

display P3 !zoo growth due to grazing !gC/day

display P4 !zoo death due to end. respiration !gC/day

display P5 !zooplankton excretion rate! gC/day

display R1 !reaction term for phytoplankton conc !gC/day

display R2 !reaction term for zooplankton conc !gC/day

display R3 !reaction term for nutrient conc !gNO3/day

display R4 !reaction term for CO2 conc !gC/day

display R5 !reaction term for organic carbon conc !gC/day

display Wup1 !upwelling rate for phytoplankton !gC/day

display Wup2 !upwelling rate for zooplankton !gC/day

display Wup3 !upwelling rate for nutrients !gNO3/day

display Wup4 !upwelling rate for CO2 !gC/day

display Wup5 !upwelling rate for organic carbon !gC/day

display Wdown1 !downwelling rate for phytoplankton !gC/day

display Wdown2 !downwelling rate for zooplankton !gC/day

display Wdown3 !downwelling rate for nutrients !gNO3/day

display Wdown4 !downwelling rate for CO2 !gC/day

display Wdown5 !downwelling rate for organic carbon !gC/day

display EUC1 !horizontal advective rate into deep - phyt conc !gC/day

display EUC2 !horizontal advective rate into deep - zoo conc !gC/day

display EUC3 !horizontal advective rate into deep - nutrient conc !gNO3/day

display EUC4 !horizontal advective rate into deep - CO2 conc !gC/day

display EUC5 !horizontal advective rate into deep - organic C conc !gC/day

display OUT1 !horizontal advection out of surface - phyt conc !gC/day

display OUT2 !horizontal advection out of surface - zoo conc !gC/day

display OUT3 !horizontal advection out of surface - nutrient conc !gNO3/day

display OUT4 !horizontal advection out of surface - CO2 conc !gC/day

display OUT5 !horizontal advection out of surface - organic Carbon !gC/day

display Fsa !flux of CO2 between surface layer and atmosphere !g/day

display Fae !flux of CO2 out of atmospheric layer to rest of Earth's atm !g/day

display CO2atm !atmospheric stock of CO2 !gC

display PCO2 !partial pressure of co2 in atmosphere !atm

display PHYTs !phyt stock in the surface !gC
display ZOOS !zoo stock in the surface !gC
display NUTs !nutrient stock in the surface !gNO3
display CO2s !CO2 stock in the surface !gC
display ORGCs !organic carbon stock in the surface !gC

display PHYTdeep !phyt stock in deep layer !gC
display ZOOdeep !zoo stock in deep layer !gC
display NUTdeep !nutrient stock in deep layer !gNO3
display CO2deep !CO2 stock in deep layer !gC
display ORGCdeep !organic carbon stock in deep layer !gC

display PHYTsconc !phyt conc in the surface !gC/m3
display ZOOSconc !zoo conc in the surface !gC/m3
display NUTsconc !nutrient conc in the surface !gNO3/m3
display CO2sconc !CO2 conc in the surface !gC/m3
display ORGCsconc !organic carbon conc in the surface !gC/m3

display PHYTdconc !phyt conc in deep layer !gC/m3
display ZOODconc !zoo conc in deep layer !gC/m3
display NUTdconc !nutrient conc in deep layer !gNO3/m3
display CO2dconc !CO2 conc in deep layer !gC/m3
display ORGCdconc !organic carbon conc in deep layer !gC/m3

display CO2atm !CO2 stock in the atmosphere !gC
display CO2atmconc !CO2 conc in the atmosphere !gC/m3

Listing of model source code

macro userderivativesection
!DERIVATIVE SECTION

!PHYT GROWTH RATE TERMS
 $SS = K_e + (K * ((PHYTs * 1000) / Vs))$
 $GSAT = (K1 * temp) * PHYTs$
 $LT = ((2.718 * f) / (SS * DPTH)) * (EXP(-(I_o / I_s)) * EXP(-(SS * DPTH))) - (exp(-(I_o / I_s)))$
 $LIMNUT = NUTs / (KM + NUTs)$

!PROCESS RATES
 $P1 = GSAT * LT * LIMNUT$
 $P2 = K2 * temp * PHYTs$
 $P3 = ((CG * ZOOS * PHYTs) * (PHYTs / (KMP + PHYTs))) / Vs$
 $P4 = K3 * temp * ZOOS$
 $P5 = ((CG * ZOOS * PHYTs) * (1 - (PHYTs / (KMP + PHYTs)))) / Vs$

!REACTION TERMS
 $R1 = P1 - P2 - (P3 / Y)$
 $R2 = P3 - P4 - P5$
 $R3 = ((U * P2) + (Z * P4) + (Z * P5)) - (U * P1)$
 $R4 = (P2 + P4) - P1$
 $R5 = P5$
!R1=0

!R2=0
!R3=0
!R4=0
!R5=0

!TRANSPORT TERMS

!UPWELLING

Wup1=(vWup*A*PHYTdeep)/Vdeep
Wup2=(vWup*A*ZOOdeep)/Vdeep
Wup3=(vWup*A*NUTdeep)/Vdeep
Wup4=(vWup*A*CO2deep)/Vdeep
Wup5=(vWup*A*ORGCdeep)/Vdeep
!Wup1=0
!Wup2=0
!Wup3=0
!Wup4=0
!Wup5=0

!DOWNWELLING

Wdown1=(vWdown*A*PHYTs)/Vs
Wdown2=(vWdown*A*ZOOs)/Vs
Wdown3=(vWdown*A*NUTs)/Vs
Wdown4=(vWdown*A*CO2s)/Vs
Wdown5=(vWdown*A*ORGCs)/Vs
!Wdown1=0
!Wdown2=0
!Wdown3=0
!Wdown4=0
!Wdown5=0

!HORIZONTAL ADVECTION INTO DEEP LAYER

EUC1=Qin*PHYTin
EUC2=Qin*ZOOin
EUC3=Qin*NUTin
EUC4=Qin*CO2in
EUC5=Qin*ORGCin
!EUC1=0
!EUC2=0
!EUC3=0
!EUC4=0
!EUC5=0

!HORIZONTAL ADVECTION OUT OF THE SURFACE LAYER

OUT1=(Qout*(PHYTs/Vs))
OUT2=(Qout*(ZOOs/Vs))
OUT3=(Qout*(NUTs/Vs))
OUT4=(Qout*(CO2s/Vs))
OUT5=(Qout*(ORGCs/Vs))
!OUT1=0
!OUT2=0
!OUT3=0
!OUT4=0
!OUT5=0

!CO2 EQUILIBRIUM FLUX BETWEEN THE OCEAN AND THE ATMOSPHERE

$$PCO2=(CO2atm/Vatm)*(1/pureCO2)$$

$$Fsa=((PCO2*HC*MMCO2)-(CO2s/Vs))*(D/A)*Vatm \text{ !if -, toward atm.; if +, toward ocean}$$

$$Fae=((HD*((co2econc/1000)-(CO2atm/Vatm)))/Ax)*Vatm \text{ !if +, toward local atm; if -, toward rest of earth's atm}$$

!STOCKS IN SURFACE LAYER

$$dPHYTs=Wup1-(Wdown1+OUT1)+R1$$

$$dZOOs=Wup2-(Wdown2+OUT2)+R2$$

$$dNUTs=Wup3-(Wdown3+OUT3)+R3$$

$$dCO2s=Wup4-(Wdown4+OUT4+Fsa)+R4$$

$$dORGCs=Wup5-(Wdown5+OUT5)+R5$$

$$\text{!liminth}(PHYTs=dPHYTs, iPHYTs, minconc, maxconc)$$

$$\text{!liminth}(ZOOs=dZOOs, iZOOs, minconc, maxconc)$$

$$\text{!liminth}(NUTs=dNUTs, iNUTs, minconc, maxconc)$$

$$\text{!liminth}(CO2s=dCO2s, iCO2s, minconc, maxconc)$$

$$\text{!liminth}(ORGCs=dORGCs, iORGCs, minconc, maxconc)$$

$$PHYTs=integ(dPHYTs, iPHYTs)$$

$$ZOOs=integ(dZOOs, iZOOs)$$

$$NUTs=integ(dNUTs, iNUTs)$$

$$CO2s=integ(dCO2s, iCO2s)$$

$$ORGCs=integ(dORGCs, iORGCs)$$

!STOCKS IN DEEP LAYER

$$dPHYTdeep=EUC1+Wdown1-(Wup1)+R1$$

$$dZOOdeep=EUC2+Wdown2-(Wup2)+R2$$

$$dNUTdeep=EUC3+Wdown3-(Wup3)+R3$$

$$dCO2deep=EUC4+Wdown4-(Wup4)+R4$$

$$dORGCdeep=EUC5+Wdown5-(Wup5)+R5$$

$$\text{!liminth}(PHYTdeep=dPHYTdeep, iPHYTdeep, minconc, maxconc)$$

$$\text{!liminth}(ZOOdeep=dZOOdeep, iZOOdeep, minconc, maxconc)$$

$$\text{!liminth}(NUTdeep=dNUTdeep, iNUTdeep, minconc, maxconc)$$

$$\text{!liminth}(CO2deep=dCO2deep, iCO2deep, minconc, maxconc)$$

$$\text{!liminth}(ORGCdeep=dORGCdeep, iORGCdeep, minconc, maxconc)$$

$$PHYTdeep=integ(dPHYTdeep, iPHYTdeep)$$

$$ZOOdeep=integ(dZOOdeep, iZOOdeep)$$

$$NUTdeep=integ(dNUTdeep, iNUTdeep)$$

$$CO2deep=integ(dCO2deep, iCO2deep)$$

$$ORGCdeep=integ(dORGCdeep, iORGCdeep)$$

!STOCK OF CO2 IN ATMOSPHERE

$$dCO2atm=+Fae-Fsa+R4$$

$$CO2atm=integ(dCO2atm, iCO2atm)$$

$$CO2atmconc=CO2atm/Vatm$$

!CONCENTRATIONS IN THE SURFACE LAYER

$$PHYTsconc=PHYTs/Vs$$

$$ZOOsconc=ZOOs/Vs$$

$$NUTsconc=NUTs/Vs$$

$CO2sconc=CO2s/Vs$
 $ORGCsconc=ORGCs/Vs$

!CONCENTRATIONS IN THE DEEP LAYER

$PHYTdconc=PHYTdeep/Vdeep$
 $ZOOdconc=ZOOdeep/Vdeep$
 $NUTdconc=NUTdeep/Vdeep$
 $CO2dconc=CO2deep/Vdeep$
 $ORGCdconc=ORGCdeep/Vdeep$

macro end